SYNTHESIS AND PROPERTIES OF TITANIA NANOFIBERS BY ELECTROSPINNING METHOD

Library
Instructional Resources Centre Ubon Ratchathani University

SERT KIENNORK

A THESIS SUBMITTED IN PARTIAL FULFILLMENT OF THE
REQUIREMENTS FOR THE DEGREE OF DOCTOR OF PHILOSOPHY
MAJOR IN PHYSICS
FACULTY OF SCIENCE
UBON RATCHATHANI UNIVERSITY
ACADEMIC YEAR 2016

COPYRIGHT OF UBON RATCHATHANI UNIVERSITY

UBON RATCHATHANI UNIVERSITY
THESIS APPROVAL
DOCTOR OF PHILOSOPHY
IN PHYSICS FACULTY OF SCIENCE

TITLE SYNTHESIS AND PROPERTIES OF TITANIA NANOFIBERS BY ELECTROSPINNING METHOD

AUTHOR MR. SERT KIENNORK

EXAMINATION COMMITTEE

ASST. PROF.DR. TOSAWAT SEETAWAN	CHAIRPERSON
ASST. PROF. DR. UDOM TIPPARACH	MEMBER
ASSOC. PROF. DR. SUPAKORN PUKIRD	MEMBER

ADVISOR

....

(ASST. PROF. DR. UDOM TIPPARACH)

....

(ASSOC. PROF. DR. UTITH INPRASIT)
DEAN, FACULTY OF SCIENCE

....

(ASSOC. PROF. DR. ARIYAPORN PONGRAT)
VICE PRESIDENT
FOR ACADEMIC AFFAIRS

COPYRIGHT OF UBON RATCHATHANI UNIVERSITY

ACADEMIC YEAR 2016

ACKNOWLEDGEMENTS

I am also grateful especially to Assist. Prof. Dr. Udom Tipparach my suporvisure, for his kindness, valuable suggestion, thesis discussions and planning the doctoral program study, who gave motivation and opportunity to me to open up my eyes in the real physics and nano material that I have never known. I would like to thanks Assoc. Prof. Dr. Supakorn Pukird, Assist. Prof. Dr. Tanin Nutaro, Dr. Vatcharinkorn Mekla and Mr. Ronariddh Nakhowong for their helpful ideas and valuable suggestions throughout this study. I would also like to thank my examining committee members for their useful suggestions.

Furthermore, I would like to express my sincere thanks to the Department of Physics, Ubon Ratchathani University and the Program of Physics, Ubon Ratchathani Rajabhat University, for supporting all my studies.

Finally, I would like to express special thank to my family, relative and friends, whose love, patience and understanding helped me to success this study.

Sert Kiennork
Researcher

บทคัดย่อ

ชื่อเรื่อง : การสังเคราะห์และสมบัติของเส้นใยนาโนไททาเนียโดยวิธีอิเล็กโตรสปินนิ่ง
ผู้วิจัย : เสริฐ เขียนนอก
ชื่อปริญญา : ปรัชญาดุษฎีบัณฑิต
สาขาวิชา : ฟิสิกส์
อาจารย์ปรึกษา : ผู้ช่วยศาสตราจารย์ ดร.อุดม ทิพราช
คำสำคัญ : ไททาเนียมไดออกไซด์, วิธีโซลเจล, เส้นใยนาโน, อิเล็กโตรสปินนิ่ง

เส้นใยนาโนไททาเนียได้ถูกสังเคราะห์ด้วยกระบวนการร่วมระหว่างโซลเจลกับกระบวนปั่นเส้นใยด้วยไฟฟ้าสถิต และกระบวนการแคลไซน์ โดยโซลเจลเตรียมจากไททาเนียมไอโซโพรพอกไซด์ และพอลิไวนิลไพโรลิโดนได้ถูกใช้เป็นสารตั้งต้น เส้นใยนาโนที่สังเคราะห์ได้ถูกนำศึกษาสมบัติเสถียรภาพทางความร้อนด้วยเทคนิค Thermogravimetric analysis (TGA) หมู่ฟังก์ชันทางเคมีด้วยเทคนิคฟูเรียร์ทรานฟอร์มอินฟราเรดสเปกโทรสโคปี (Fourier transform infrared spectroscopy, FTIR) โครงสร้างผลึกด้วยเทคนิคการเลี้ยวเบนรังสีเอกซ์ (X-ray diffraction, XRD) และลักษณะสัณฐานวิทยาด้วยเทคนิคกล้องจุลทรรศน์อิเล็กตรอนแบบส่องกราด (Scanning electron microscopy, SEM) ผลการวิจัยพบว่าเส้นโค้ง TGA แสดงให้เห็นว่าตัวทำละลาย สารอินทรีย์ พอลิเมอร์ เกิดการสลายที่อุณหภูมิประมาณ 100°C, 300°C และ 350-400°C หรือสูงกว่า ตามลำดับ หลังจากที่เตรียมได้เส้นใยนาโนก่อนเผามีลักษณะพื้นผิวที่เรียบ ยาวต่อเนื่อง วางเรียงตัวกันแบบสุ่มและมีเส้นผ่านศูนย์กลางในช่วง 298 -365 nm เส้นผ่าศูนย์กลางของเส้นใยจะลดลงเมื่อเพิ่มเมื่ออุณหภูมิการแคลไซด์เพิ่มสูงขึ้น หลังจากเผาแคลไซน์ พบว่าเส้นใยนาโนไททาเนียที่มีลักษณะพื้นผิวค่อนข้างขรุขระและมีขนาดเส้นผ่านศูนย์ลดลงอยู่ในช่วง 147- 284 nm หลังจากเผาแคลไซน์ที่อุณหภูมิ 600°C เป็นเวลา 1 ชั่วโมง โครงสร้างเส้นใยนาโนไททาเนียที่เกิดขึ้นเมื่อเผาแคลไซน์ที่อุณหภูมิ 500°C เป็นเฟสเป็นอนาเทสและรูไทล์ 600-700°C มีเฟสรูไทล์เพิ่มขึ้น และที่ 700°C มีเฟสรูไทล์อย่างสมบูรณ์ หมู่ฟังก์ชันของเส้นใยนาโนไททาเนียมีแถบการดูดกลืนในช่วง 500-700 ต่อเซนติเมตรซึ่งยืนยันโลหะออกไซด์ของเส้นใยนาโนไททาเนีย

ABSTRACT

TITLE	: SYNTHESIS AND PROPERTIES OF TITANIA NANOFIBERS BY ELECTROSPINNING METHOD
AUTHOR	: SERT KIENNORK
DEGREE	: DOCTOR OF PHILOSOPHY
MAJOR	: PHYSICS
ADVISOR	: ASST. PROF. UDOM TIPPARACH, Ph.D.
KEYWORDS	: TITANIUM DIOXIDE, SOL-GEL METHOD, NANOFIBERS, ELECTROSPINNING

Titania (TiO_2) nanofibers were synthesized by combinations of sol-gel assisted electrospinning and calcination processes. The sol-gel was prepared from titanium (IV) isopropoxide (TIP) and poly (vinylpyrrolidinone) (PVP). The synthesized TiO_2 nanofibers were investigated in various ways: thermal stability by thermogravimetric analysis (TGA), functional groups by Fourier transform infrared spectroscopy (FTIR), crystalline structures by X-ray diffraction (XRD), and surface morphology by scanning electron microscopy (SEM). The TGA curve revealed that the volatile solvents, organic precursor, and polymer were completely removed at approximately 100, 300, and 350-400 °C or higher respectively. The as-spun TIP/PVP fibers were smooth surfaced, uniform, and continuous with average diameters of 298-365 nm. The diameter of the nanofibers decreased with increasing calcination temperature. The nanofibers calcined at 600 °C and became rough with diameters of 147-284 nm. The phases of TiO_2 nanofibers calcined at 500 °C were anatase and rutile. After increasing calcination to 600-700 °C, the nanofibers became more rutile phase, and above 700 °C the nanofibers became rutile phase completely. The FTIR spectra showed absorption bands at 500-700 cm^{-1} that confirmed the formation of metal-oxide of titania nanofibers.

CONTENT

PAGE

ACKNOWLEDGMENT **I**
THAI ABSTRACT **II**
ENGLISH ABSTRACT **III**
CONTENTS **IV**
LIST OF TABLES **VI**
LIST OF FIGURES **VII**
CHAPTER 1 INTRODUCTION
1.1 Introduction 1
1.2 Research Objectives 3
1.3 Scope of research 3
1.4 Benefits of this research 3
CHAPTER 2 THEORY BACKGROUND LITERATURE REVIEW
2.1 Nanomaterials 4
2.2 One-dimensional nanostructures 5
2.3 Titanium dioxide 5
2.4 Sol-gel process 10
2.5 Electrospinning process 12
CHAPTER 3 EXPERIMENTAL METHOD
3.1 Materials 15
3.2 Preparation of TiO_2/PVP solution 15
3.3 Electrospinning apparatus 16
3.4 Experimental Procedures 17
3.5 Characterization techniques 18
CHAPTER 4 RESULS AND DISCUSSION
4.1 Calcination of the TiO_2/PVP composite fibers 23
4.2 Crystal structure of thetitania nanofibers 24
4.3 Surface Analysis of the titania nanofibers 28
4.4 Fourier transforms infrared spectroscopy of the titania nanofibers 32

CONTENT (CONTINUED)

PAGE

CHAPTER 5 CONCLUSIONS AND SUGGESTION
5.1 Summary 34
5.2 Conclusions 34
5.3 Suggestions 35
REFERENCES **36**
APPENDIX **42**
CURRICULUM VITAE **51**

LIST OF TABLES

TABLE **PAGE**

4.1 Calculation of the crystallite size of the PVP/TIP composite nanofibers at amount of 1.0, 5.0 and 10.0 mmol calcined at 600°C for 1 h 27

4.2 Calculation of the crystallite size of TiO_2 nanofibers with the content of TIP 5.0 mmol calcined at 500, 600, and 700°C for 2 h 28

LIST OF FIGURES

FIGURE **PAGE**

2.1 Density of states for bulk (3D blue), quantum well (2D red), quantum wire (1D green) and quantum Dot (0D black) 5

2.2 Structure models of rutile (a), anatase (b), and brookite (c) polymorphs of TiO_2. The crystal structures of anatase (b) and brookite (c) are viewed along (010) and Approximate (001) directions, respectively 7

2.3 XRD patterns of the TiO_2 crystal structure composite fibers calcined in air then preserved heat in different atmospheres 8

2.4 the example of SEM micrographs of TiO_2/PVP composite nanofibers. (A) As-spun nanofibers. (B–G) are TiO_2 nanofibers calcined in air for 3 h at 300-800 °C. (Scale bar is 500 nm) 9

2.5 a schematic diagram showing the process of electrospinning 13

3.1 Schematic drawing for preparation of TIP/PVP solution 16

3.2 Schematic drawing of the electrospinning setup 17

3.3 (a) Schematic of the SEM and (b) electron beam-example interaction 20

4.1 TGA curve of PVP/TIP composite nanofibers at heating rate 10°C min−1 in oxygen gas 24

4.2 XRD patterns of (a) PVP /TIP composite nanofibers, (b) PVP/TIP1.0, (c) PVP/TIP 5.0 and (d) PVP/TIP 10 mmolcalcined at 600°C for 1 h 25

4.3 XRD patterns of TiO_2 nanofibers with the content of TIP 5.0 mmol calcined at (a) 500, (b) 600, and (c) 700°C for 2 h 26

4.4 SEM images of the PVP/TIP composite fiber of as-spun nanofibers; PVP/TIP 1.0 mmol 29

4.5 SEM images of the PVP/TIP composite fiber of as-spun nanofibers; PVP/TIP 5.0 mmol 30

4.6 SEM images of the PVP/TIP composite fiber of as-spun nanofibers; PVP/TIP 10.0 mmol 30

LIST OF FIGURES (CONTINUED)

FIGURE		PAGE
4.7	SEM images of the PVP/TIP composite fiber of as-spun nanofibers; PVP/TIP 1.0 mmol calcined at 600°C for 1 h	31
4.8	SEM images of the PVP/TIP composite fiber of as-spun nanofibers; PVP/TIP 5.0 mmol calcined at 600°C for 1 h	31
4.9	SEM images of the PVP/TIP composite fiber of as-spun nanofibers; PVP/TIP 10.0 mmol calcined at 600 °C for 1 h	32
4.10	FTIR spectrums for (a) as-spun PVP/TIP nanofibers and (b) TiO_2 nanofibers calcined at 600°C for 1 h	33

CHAPTER 1
INTRODUCTION

In this chapter, I introduce and overview of the background and state of research for preparation and characterization of electrospunTiO_2 nanofibers by electrospinning. I also introduce my research plan, objective, and thesis expectation.

1.1 Introduction

Titanium dioxide, titanium (IV) oxide or titania (TiO_2) is one of the most popular materials for a variety of the applications in self-cleaning coating (superhydrophobic/ superhydrophilic/superamphiphobic), photocatalysis, Li-ion batteries, dye-sensitized solar cells, photocatalysis, etc[1, 2]. Titanium dioxide, a key semiconductor with a wide bandgap, offers high exciton binding energy, tunable crystal structure, low absorption coefficient, high refractive index and effective photocatalytic activity [2, 3]. TiO_2 can be found in three different crystalline forms: anatase, rutile, and brookite, and the ban gaps of these three TiO_2 phases are 3.0, 3.2, and 3.25 eV, respectively [4]. The nanostructures that are defined as having at least one dimension between 1 and 100 nm have received steadily growing interests as aresult of their peculiar and fascinating properties, and applications superior to their bulk counterparts [5]. Within the last decade, one-dimensional (1D) nanostructured materials such as nanofibers, nanowires, nanorods, nanowiskers, nanobelts, and nanotubes have attracted attention due to their unique properties and wide range of potential applications [6]. It is general believed that 1D nanostructures provide a good system to investigated the dependence of electrical and thermal transport or mechanical properties on dimensionality and size reduction (or quantum confinement) [6]. They are also expected to play an important role as both interconnects and functional units in fabricating electronic, optoelectronic, electrochemical, and electromechanical devices with nanoscale dimensions. Nanomaterials have very high surface areas to volume ratios, which result in special properties in comparison to bulk materials [7]. There are many kinds of nanoscale materials including nanoparticles, nanopowders, nanorods, nanotubes, and nanowires. Nanomaterials may be zero-dimensional (e.g. nanoparticles), one-dimensional (e.g. nanorods or nanotubes), or two-dimensional (usually realized as thin films or stack of thin films) [8]. 1D nanostructure has the advantages including high aspect ratio, high interfacial area, porosity and shortest pathways for ion diffusion compare other nanostructure [9]. 1D nanomaterials can be prepared by many methods such as template-directed methods, vapor-phase methods, interface synthesis techniques, solvothermal synthesis, solution-phase growth controlled by capping reagents, nanolithography, and self-assembly [10]. However, each of these methods has limitations, such as materials restrictions, high cost, and high process complexity. Recently, electrospinning is a simple, versatile, and relatively inexpensive technique for synthesis of ultrafine fibers down to a few nanometers and of a broad range of complex architectures of nanofibers and nonwovens [11]. It has been used to make nanofibers, nanotubes, nanobelts, nanotube, and porous membranes. The morphology and properties of nanofibers depend on molecular weight. However, the creation of ultrafine nanofibers requires the careful consideration of many operating parameters (such as polymer molecular weight, applied voltage, solution feedrate and spinning distance), environmental parameters (such astemperature, humidity and air velocity in the chamber) and solution properties (such as conductivity, viscosity and surface tension) [12]. In typical process of electrospinning, an electrical potential is applied between a droplet of a polymer solution, or melt, held at the end of a capillary tube and grounded target. When the applied electric field overcomes the surface tension of the droplet, a charged jet of polymer solution is ejected. The jet exhibits bending instabilities caused by repulsive forces between the charges carried with the jet. The jet extends through spiraling loops; as the loops increase in diameter the jet grows longer and thinner until it solidifies or collects on the target.The solvent in the polymer jet evaporates during its travel to the collecting screen [13]. Recently, the synthesis of TiO_2 were prepared by various technique such as sol-gel method [14], sputtering method [5], co-precipitation method [16], anodization [17] and electrospinning method [18].

In this work, TiO_2 nanofibers were prepared by sol-gel assisted electrospinning. The metal source ratio, calcination temperature were investigated in detail to understand the situation condition for the synthesis and properties of TiO_2 nanofibers. The TiO_2 nanofibers were characterized by thermogravimetric analysis (TGA), Fourier transform infrared spectroscopy (FTIR), X-ray diffraction (XRD), and scanning electron microscopy (SEM).

1.2 Research Objectives

1.2.1 To synthesize of TiO_2 nanofibers by electrospinning.

1.2.2 To study the effects of concentration of Ti source/PVP ratio (titanium (IV) isopropoxide ($Ti(OCH(CH_3)_2)_4$/polyvinylpyrrolidone), and calcination temperature on crystalline phase, surface morphology of TiO_2 nanofibers.

1.2.3 To investigate the crystalline phases, diameter sizes, surface morphology, chemical structure and bonds, and thermal properties of TiO_2 nanofibers by thermogravimetric analysis (TGA), Fourier transforms infrared spectroscopy (FTIR), X-ray diffraction (XRD), and scanning electron microscopy (SEM).

1.3 Scope of research

1.3.1 To investigate the effects of metal source: PVP ratios.

1.3.2 To study the effects of different calcination temperatures and times.

1.3.3 Characterize the physical properties and chemical structure and bonds of TiO_2 nanofibers.

1.4 Benefits of this research

1.4.1 Able to synthesize of one-dimensional TiO_2 nanofibers with diameter in nanoscale by electrospinning.

1.4.2 Able to application of TiO_2 nanofibers by electro spinning with sol-gel.

CHAPTER 2

THEORY BACKGROUND LITERATURE REVIEW

In this chapter, I review the theoretical background of nanomaterials and describe the basic theory and properties of titania such as structure and general properties of titania, sol-gel process and electrospinning process. Furthermore, I present literature survey of the previous works related to this work.

2.1 Nanomaterials

Nanomaterials are currently attracting much interest due to their properties for applications in nanotechnology. The properties of nanomaterials depend on their morphology. Two major effects of nanostructure materials are the size dependent effect and the high surface to volume ratio. Firstly due to size dependent effect, the properties of nanostructures are different from that of the bulk. For example, density of state (DOS) at different size dependent the different functions are shown in Figure 2.1. For 3 dimensions, DOS is a continuous function with respect to energy and is related to square root of energy. For 2, 1 and 0 dimensions, the DOSs is discrete function with respect to energy. The lower the size dependent, the smaller the number of available energy value and the discrete function turns into a delta function at zero dimensions. Secondly the high surface to volume ratio of nanostructure refers normally to the field of surface science. Surface science is the study of physics phenomena that occur at the interface of two phases, including solid - liquid interfaces, solid - gas interfaces, solid - vacuum interfaces and liquid - gas interfaces. Some related practical applications are classed as surface engineering.

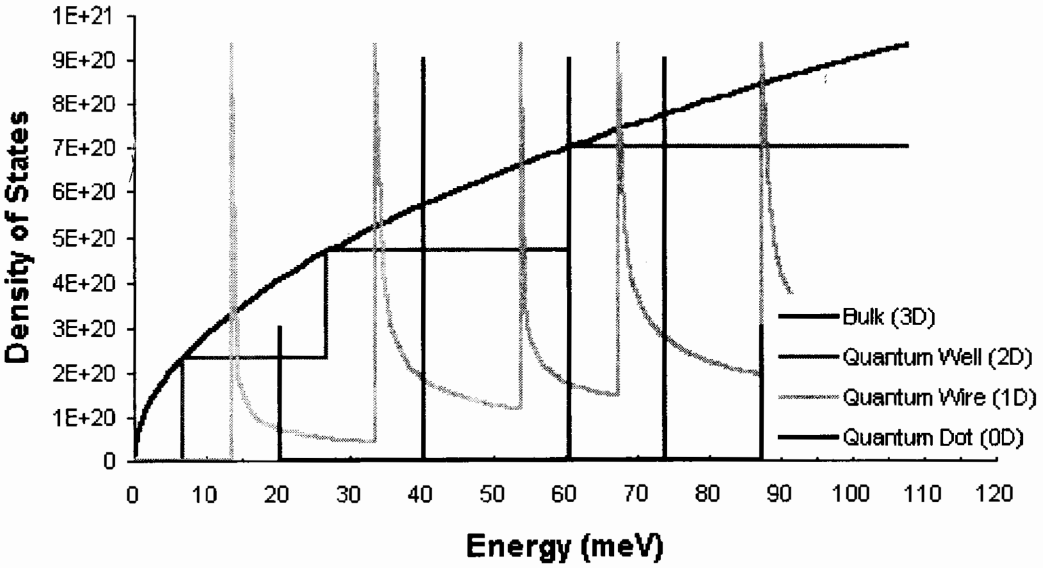

Figure 2.1 Density of states for bulk (3D blue), quantum well (2D red), quantum wire (1D green) and quantum Dot (0D black) [15]

2.2 One-dimensional nanostructures

One-dimensional nanostructures (1D) have various forms including nanowhiskers, nanofibers, nanowires and nanorods. In many cases, nanotubes and nanocables are also considered 1D structures. Although nanowhiskers and nanorods are in general considered to be shorter than fibers and nanowires, the definition is often a little arbitrary. In addition, 1D structures with diameters ranging from several nanometers to several hundred microns were referred to as whiskers and fibers in the early literature, whereas nanowires and nanorods with diameters not exceeding a few hundred nanometers are used predominantly in the recent literature.

2.3 Titanium dioxide

Titanium dioxide (TiO_2) nanomaterials have been much attention due to technological applications including pigments, cosmetics, ultrathin capacitors, photovoltaic cells, and photocatalysis. The crystalline polymorphs have three most commonly encountered crystalline polymorphs such as anatase, brookite, and rutile. All the three crystal structures are made up of distorted TiO_6 octahedral, but in different ways [16].

The scientifically and technologically most relevant modifications of titanium dioxide are anatase, rutile and brookite, which have the following crystallographic properties:

(1) anatase (space group $I4_1/amd$, symmetry D_{4h})
(2) rutile (space group $P4_2/mnm$, symmetry D_{4h})
(3) brookite (space group Pbca, symmetry D_{2h})

Other modifications, that have been synthesized, are [17]

(4) TiO_2 II ("columbite", (α-PbO_2) space group Pbcn),
(5) TiO_2 III ("baddeleyite", space group $P2_1/c$)
(6) TiO_2 (H) ("hollandite", space group I4/m),
(7) TiO_2 (R) ("ramsdellite", space group Pbnm)
(8) TiO_2 (B) ("bronze", space group C2/m) Except TiO_2 (B), none of the latter modifications occur in nature. They have been mostly synthesized by high pressure treatment of anatase or rutile.

Formally, titanium dioxide is made up of d^0 titanium ions (charge +IV) at the center of an octahedron of six O^{2-} ions. The most important modifications anatase and rutile mainly differ by the distortion inside the octahedron. The unit cell of anatase and rutile are shown in Figure. 2.2. Anatase has a density of 3.8 – 4.0 g/cm^3, which is a little bit less than rutile with a density of 4.2 - 4.3 g/cm^3. The average distance between the Ti^{4+} ions in anatase is smaller compared to rutile, which makes it thermodynamically less stable. Hartree-Fock calculations [18] have shown that the enthalpy of formation is about 1.2 - 2.8 kcal higher for anatase. However, the phase transition from anatase to rutile needs a significant thermal activation and occurs between 700 - 1000 °C depending on the crystal size and the impurity content [19].

The practical application of TiO_2 strongly depends upon the crystalstructure, morphology, and size of the crystallites. Each crystalline modification of TiO_2 has different physiochemical properties, such as density, refractive index, and photochemical reactivity. Rutile has the highest density and refractive index among the three phases and therefore has been widely employed in pigments and cosmetics industries. Anatase generally shows better performances than its rutile counterpart in photocatalytic applications, likely due to the longer lifetime of the photo-excited h+/e- carriers in the anatase lattice. The brookite phase is the least

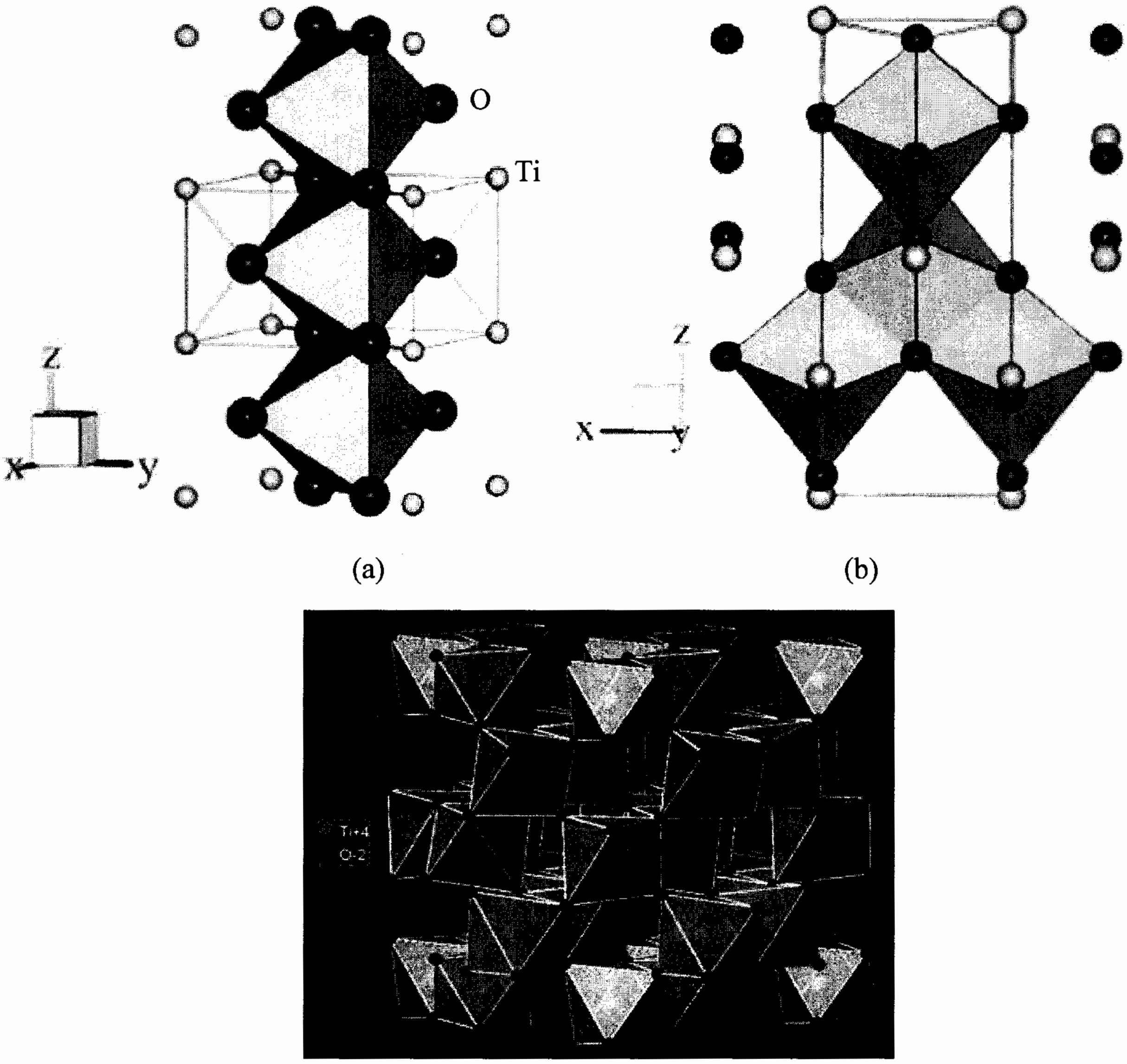

(a) (b)

(c)

Figure 2.2 Structure models of rutile (a), anatase (b), and brookite (c) polymorphs of TiO_2. The crystal structures of anatase (b) and brookite (c) are viewed along (010) and Approximate (001) directions, respectively [20].

studied in many aspects of its properties, mainly owing to the difficulties encountered in obtaining its pure form. Size, shape, and phase structure controlled synthesis of TiO_2

For example, the XRD patterns obtained, no obvious doping related peaks appeared despite the doped samples showing characteristic TiO_2 peaks, which may be due to the lower concentration of the doped species under nitrogen atmosphere. Moreover, the limited amount of dopants may be moved to either interstitial positions or the substitutional sites of the TiO_2 crystal structure. The XRD patterns of composite fibers calcined at different temperatures (500°C, 550°C, 600°C, and 650 °C)[21] as shown in Figure 2.3

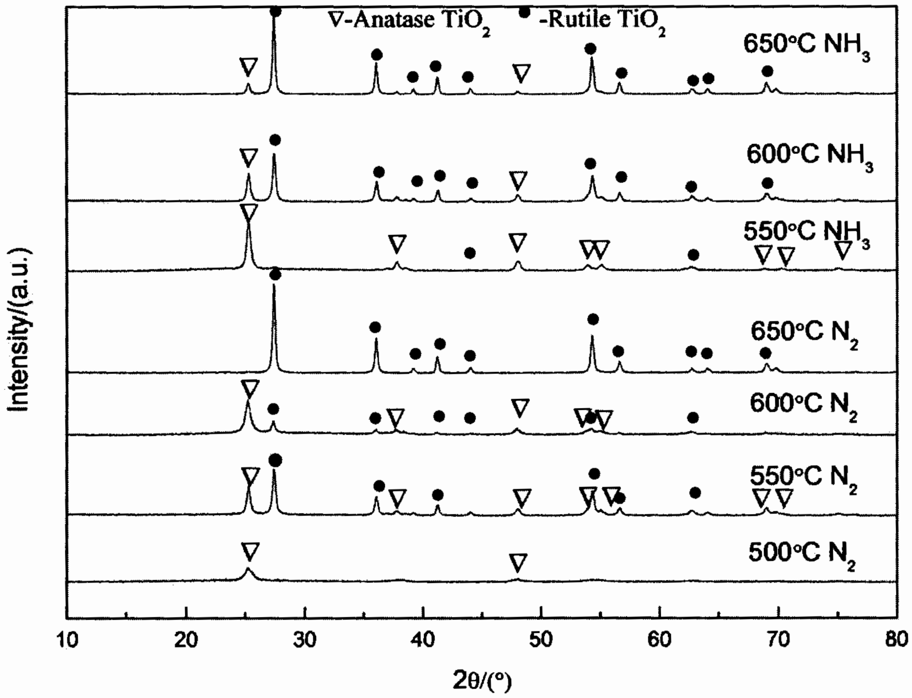

Figure 2.3 XRD patterns of the TiO_2 crystal structure composite fibers calcined in air then preserved heat in different atmospheres [21].

Morphology, that is, the study of form comprising shape, size, and structure, is important for TiO_2 research in general. For nanostructured TiO_2, popularly known as TiO_2 nanomaterials, morphology has special significance since form, in this case, dictates physical and chemical properties [22, 23]. Unlike bulk of TiO_2, properties of TiO_2 nanomaterials are strongly correlated to shape. This shape is attained during growth through a self-assembling process dictated by the interplay of size and molecular interactions [23, 24]. Deviations from bulk properties become prominent as the size of TiO_2 nanomaterials starts to be comparable to the size of constituent molecules or to some other characteristic length scale like electron mean-free path [22]. In a typical application, one deals with a collection of TiO_2 nanomaterials, which may be dispersed in a matrix [25] forming a composite TiO_2. Properties of TiO_2 nanocomposites are controlled not only by morphology of individual TiO_2 nanomaterials, but also by the nature of interactions, which, inturn, is determined by the distribution of TiO_2 nanomaterials in the matrix [26]. For example, the morphology of the as prepared and calcined TiO_2/PVP composite nanofibers was revealed by SEM and AFM. Figure 2.4 shows the SEM micrographs of the as-prepared and calcined TiO_2/PVP composite nanofibers [27].

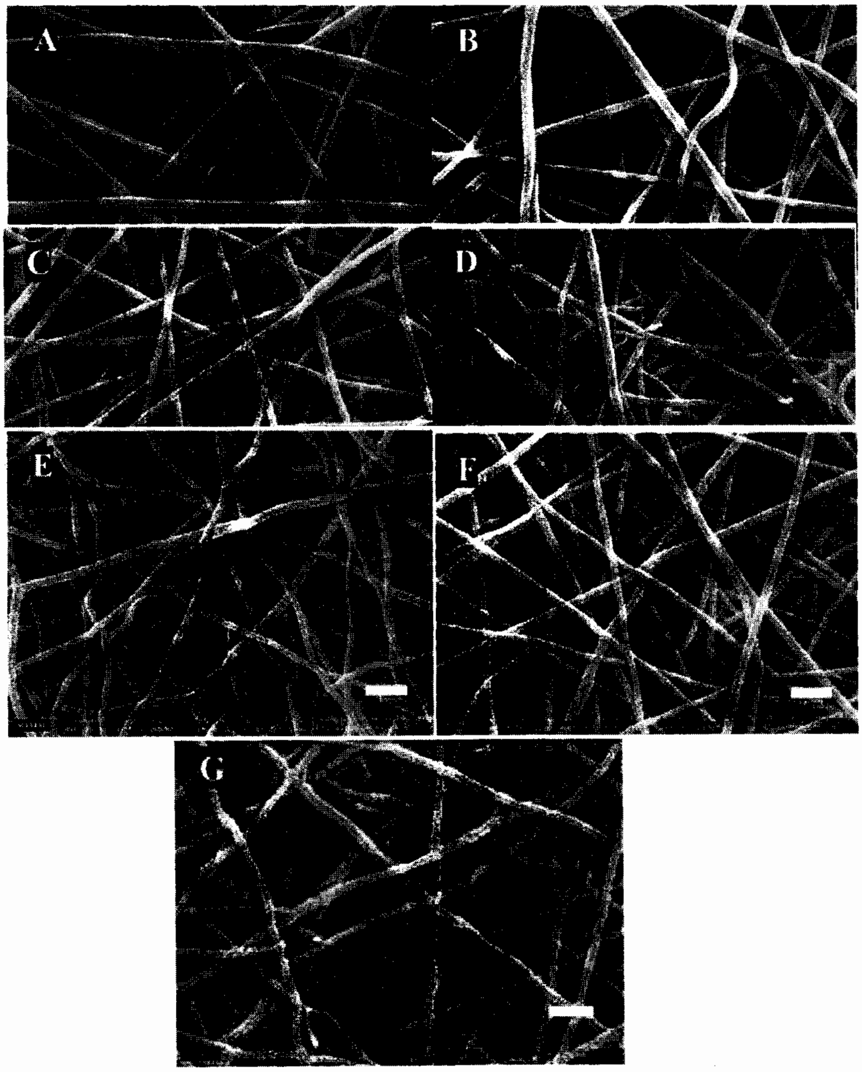

Figure 2.4 the example of SEM micrographs of TiO_2/PVP composite nanofibers. (A) As-spun nanofibers. (B–G) are TiO_2 nanofibers calcined in air for 3 h at 300-800 °C. (Scale bar is 500 nm) [27].

2.4 Sol-gel process [28]

Liquid phase synthesis precipitating nanoparticles from a solution of chemical compounds can be classified into five major categories: (1) colloidal methods, (2) sol-gel processing, (3) water – oil microemulsions method, (4) hydrothermal synthesis, and (5) polyol method. Solution precipitation relies on the precipitation of nanometer-sized particles within a continuous fluid solvent. An inorganic metal salt, such as chloride, nitride and so on, is dissolved in water. Metal cations exist in the form of metal hydrate species, for example, $Al(H_2O)^{3+}$ or $Fe(H_2O_6)^{3+}$. These hydrates are added with basic solutions, such as NaOH or Na_4OH. The hydrolyzed species condense and then washed, filtered, dried and calcined in order to obtain the final product. Sol-gel technique, sol-gel technology is a well-established colloidal chemistry technology, which offers possibility to produce various materials with novel, predefined properties in a simple process and at relatively low process cost. The sol is a name of a colloidal solution made of solid particles few hundred nm in diameter, suspended in a liquid phase. The gel can be considered as a solid macromolecule immersed in a solvent. Sol-gel process consists in the chemical transformation of a liquid (the sol) into a gel state and with subsequent post treatment and transition into solid oxide material. The main benefits of sol-gel processing are the high purity and uniform nanostructure achievable at low temperatures. The precursor in sol-gel preparation can either be a metal salt/alkoxide dissolved in an appropriate solvent or stable colloidal suspension of performed sols. Metal alkoxides have been the most extensively used because they are commercially available in high purity and their solution chemistry has been documented. At its simplest level, sol-gel chemistry with a metal alkoxides can be described in them of two classes of reaction:

$$\text{Hydrolysis: -M-OR-H2O} \longrightarrow \text{-M-OH+ROH} \qquad (2.1)$$

$$\text{Condensation: -M-OH-XO-M-} \longrightarrow \text{-M-O-M+XOH,} \qquad (2.2)$$

where X can either be H or R (an alkyl group).

Such a description oversimplifies the overall process because it does not correctly represent the molecular formulas of intermediates and end products, nor does it depicts the simultaneous occurrence of the two reactions. However, this oversimplification captures the key phenomenological idea that a three-dimensional gel network comes from the condensation of partially hydrolyzed species. Any parameter that affects either or both of these reactions is thus likely to have impact on the properties of the product. In fact, the important variables are the reaction rates of hydrolysis and condensation. Because hydrolysis and condensation are both nucleophilic displacement reactions, the reactivity of metal alkoxide depends on the positive partial charge of the metal atom and its coordination number.

The sol-gel parameters discussed so far, its effect on gel properties can often be observed by an experimental parameter known as gel time. Gel time is defined as the time that the solution undergoes rapid rise in viscosity which is corresponding to the transition from viscous fluid to elastic gel. At the gel point, the solid phase forms a continuous structure that reflects the formation and branching of particle under specific growth condition.

This particular phase is important because it is the genesis of structural evolution that takes place in all subsequent processing steps. For example, Hani-Albetran and Yu (Roger) [29] TiO_2 nanofibers were prepared within polyvinylpyrrolidone (PVP) polymer using a combination of sol–gel and electrospinning techniques. TiO_2/PVP solutions were prepared by mixing 40 wt%, 50 wt% or 60 wt% TIP with a constant mixed solvent, which comprised 2.098 g acetic acid and 4.734 g ethanol (1:3 volume ratio) with 2.05 g PVP polymer inside a glass bottle. The solutions were subsequently subjected to magnetic stirring for 120 min at 80 °C. The viscosity of the TiO_2/PVP solution depends on the concentration and molecular weight of PVP polymer, the solvent, and TiO_2 sources. As the solvent and PVP were constant, the viscosities of the solutions were solely controlled by the TIP concentration (wt %). Increasing the TiP concentration (284.22 g/mol) reduces the concentration of PVP (1,300,000 g/mol), which further reduces the solution viscosity. [30] reported on the preparation of TiO_2 nanofibers with diameters of 100 ~ 300 nm were prepared by using sol-gel and electrospun TiO_2/PVP fibers by drying at 5 h in air and subsequent annealing for 3 h at 500 °C. The precursor solution was prepared from titanium tetraisopropoxide ($Ti(OCH(CH_3)_2)_4$, 98 %, Aldrichi, USA) in ethanol by stirring. Polyvinylpyrrolidone (PVP, Mw = 1,300,000, Aldrichi, USA) dissolved in ethanol and acetic acid was added to the TiO_2 precursor solution by weight. Ethanol was used in the present study instead of water. The resistivity (viscosity) rose as alcohol was added because alcohol had a resistivity that is at least two orders of magnitude greater than that of water.

2.5 Electrospinning process

In 1934, a process was patented by Anton Formhals [31-33], where in an experimental setup was outlined for the production of polymer filaments using electrostatic force. When used to spin fibers this way, the process is termed as electrospinning.

In the electrospinning process a high voltage is used to create an electrically charged jet of polymer solution or melt, which dries or solidifies to leave a polymer fiber [34, 35]. One electrode is placed into the spinning solution/melt and the other attached to a collector. Electric field is subjected to the end of a capillary tube that contains the polymer fluid held by its surface tension. This induces a charge on the surface of the liquid. Mutual charge repulsion causes a force directly opposite to the surface tension [36]. As the intensity of the electric field is increased, the hemispherical surface of the fluid at the tip of the capillary tube elongates to form a conical shape known as the Taylor cone [37]. With increasing field, a critical value is attained when the repulsive electrostatic force overcomes the surface tension and a charged jet of fluid is ejected from the tip of the Taylor cone. The discharged polymer solution jet undergoes a whipping process [38] wherein the solvent evaporates, leaving behind a charged polymer fiber, which lays itself randomly on a grounded collecting metal screen. In the case of the melt the discharged jet solidifies when it travels in the air and is collected on the grounded metal screen.The polymer solution or melt is contained in a glass tube, usually a pipette that is connected to a syringe like apparatus. A metering pump attached to the plunger of the syringe generates a constant pressure and flow of the fluid through the pipette. The driving force is provided by a high voltage source through a wire immersed in the solution. The high voltage source can generate up to 30 kV, and the setup can be run on either positive or negative polarity. Adjusting the flow of the fluid and the magnitude of the electric field controls the spinning rate. A comprehensive mathematical model of this process was developed by Renecker et al (1996) [39]. The electrospinning process consists of three stages: (1) Jet initiation and the extension of the jet along a straight line. (2) The growth of a bending instability and the further elongation of the jet, which allows the jet to become very long and thin while its follows a looping and spiraling path. (3) Solidification of the jet into nanofibers. A schematic drawing of the electrospinning process is show in Figure.2.5

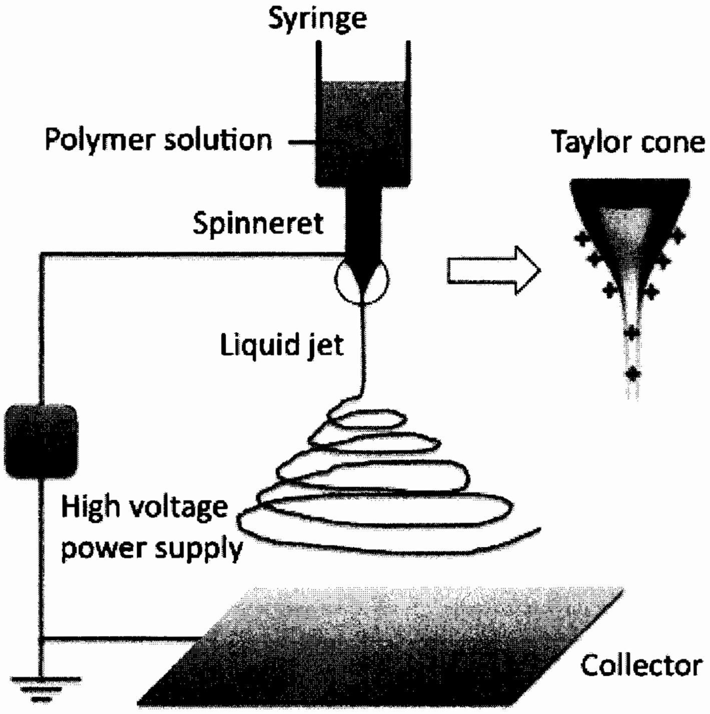

Figure 2.5 a schematic diagram showing the process of electrospinning [40].

In 2003, Li and Xia [41] first studied fabrication of titanium dioxide nanofibers by using electrospinning method with a controllable diameters and porous structure. When ethanol solution containing both poly (vinyl pyrrolidone) (PVP, M_w~1,300,000) and titanium tetraisopropoxide was injected through a needle under strong electrical field, composite nanofibers made of PVP and amorphous TiO_2 were formed (with lengths up to several centimeters) as a result of electrostatic jetting. These nanofibers could be subsequently converted into anatase without changing their morphology via calcination in air at 500 °C. The average diameter of these ceramic nanofibers could be controlled in the range from 20 to 200 nanometers.It was found that, after calcined a 500°C, the nanofibers remained in continuous structure which their average diameter reduced. This size reduction could be accounted by the loss of PVP from the nanofibers and crystallization of titanium dioxide. They also reported the following: the nanofibers increased in diameter at the PVP concentration was increased, Thinner nanofibers were obtained when the strength of the electric field (E) was increased; faster feeding rate of PVP solution often resulted in tick fibers; the use of titanium tetraisopropoxide at lower concentration led to the formation of thinner ceramic nanofibers. They believe that the electrospinning procedure described here could be extended to provide a generic route to nanofibers made of other oxides such as SnO_2, SiO_2, Al_2O_3, and ZrO_2.

Jeerapong Watthanaaruna, et al. [42] studied the effects of preparation conditions and secondary metal dopant on fabricating TiO_2/PVP composite nanofibers by combined sol-gel and electrospinning techniques. The spinning was prepared by titanium tetraisopropoxide (TIP) in ethanol mixed with acetic acid and polyvinylpyrrolidone (PVP) in ethanol. The average diameters of the pre calcined as-spun fibers were in the range of about 120–350 nm, while those of the post calcined ones were in the range of about 100–230 nm. The effects of spinning conditions were determined. Increasing PVP concentration led to an increase in the fiber diameters. Moreover, the choice of the calcination temperature has a strong influence on the crystalline phase formation of as-spun titanium dioxide fibers, with the transformation from anatase to rutile occurring more readily with increasing calcination temperature.Addition of silicon as the second metal dopant helped increase the thermal stability of the resulting titanium dioxide nanofibers.

Sudha Madhugiriet, et al. [43] have prepared electrospun mesoporous titanium dioxide fibers. The fibers contained anatase crystallized in the pore walls which transformed to rutile upon the calcination above 800°C. The electrospun fibers (calcination at 600°C, surface area of 32 m^2/g) were evaluated for the photodecomposition of phenol and formic acid comparing with two different commercial titanium dioxide samples (Degussa P25, surface area of 50 m^2/g and Hombikat UV 100, surface area 334 m^2/g). It was found that the photocatalytic property of the calcined titanium dioxide fibers fell well below those of the commercial catalysts. However, they suggested that there were several parameters including fiber size and porosity that can be tuned to improve reactivity. The titanium dioxide fibers are also being evaluated for photovoltaic applications.

Ubon Rajathanee Univ.. Instructional Resources Centre

CHAPTER 3

EXPERIMENTAL METHOD

This chapter describes the preparation of titanium dioxide nanofibers by electrospinning. It is divided into five parts: precursor, preparation of TiO_2/PVP solution and sol-gel, electrospinning apparatus, experimental procedures, and characterization of the samples.

3.1 Materials

The fabrication of titanium dioxide nanofibers using sol-gel and electrospinning technique were used to prepare with the following steps;

(1) Titanium (IV) isopropoxide (TIP) 97% was purchased from Sigma- Aldrich Chemical Company.

(2) Polyvinylpyrrolidone (PVP), $M_w \approx 1,300,000$ was purchased from Sigma-Aldrich Chemical Company.

(3) Methanol was purchased from Carlo Erba Reagents.

(4) Ethanol alcohol was purchased from Carlo Erba Reagents.

(5) Acetic acid was purchased from Carlo Erba Reagents.

All chemical reagents were received without any purification.

3.2 Preparation of TiO_2/PVP solution

In a typical procedure, based on a sol-gel processing, 1.0 mmol of TIP was dissolved in 4 mL of glacial acetic acid and 10 mL of methanol with stirring at room temperature for half an hour to get clear solution. To this solution, 1.12 g of PVP was added in TIP solution and then stirred until obtain mixture solution. Then, TIP/PVP was prepared with 5.0 and 10.0 mmol by using the same method as described above to obtain TIP/PVP solution. Schematic drawing of the preparation of TIP/PVP solution is showed in figure 3.1.

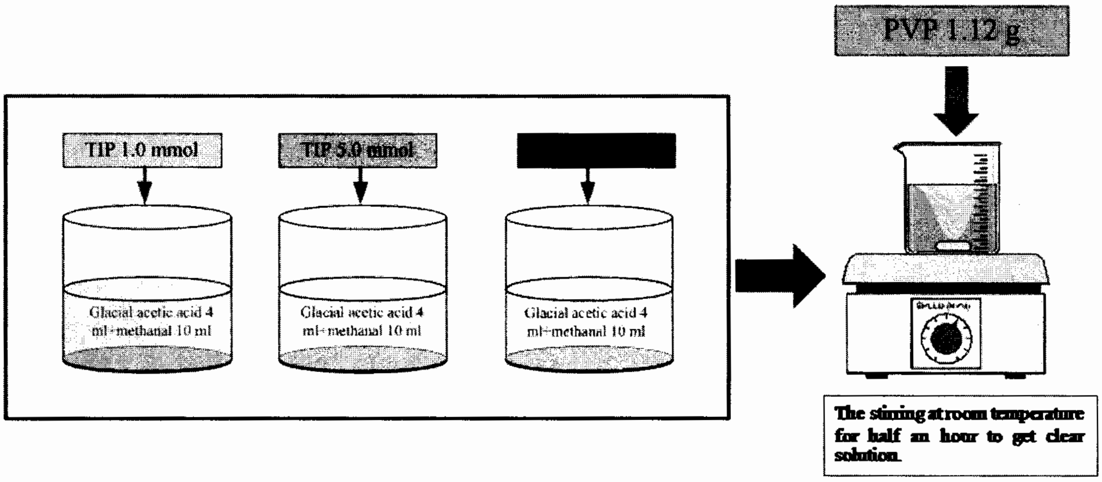

Figure 3.1 Schematic drawing for preparation of TIP/PVP solution.

3.3 Electrospinning apparatus

The schematic diagram of the electrospinning apparatus is shown in Figure 3.2. The components of the electrospinning apparatus are described as follows;

(1) A high power supply (ES30P, Gamma High Voltage Research Inc., Ormond Beach, Florida) was used to generate DC voltage from 0-30 kV, with very low electrical current of 166 microamperes,

(2) A 10 mL plastic syringe and stainless steel needle (gauge number 21, the inside diameter of 0.6 mm and the outside diameter of 0.838 mm) was used as a nozzle and as an electrode to conduct the electrical energy from a high-voltage power supply to the solution. The needle tip was cut into a flat shape to prevent the corona discharge,

(3) A copper plate was usedas a ground collector which covered with aluminum foil.

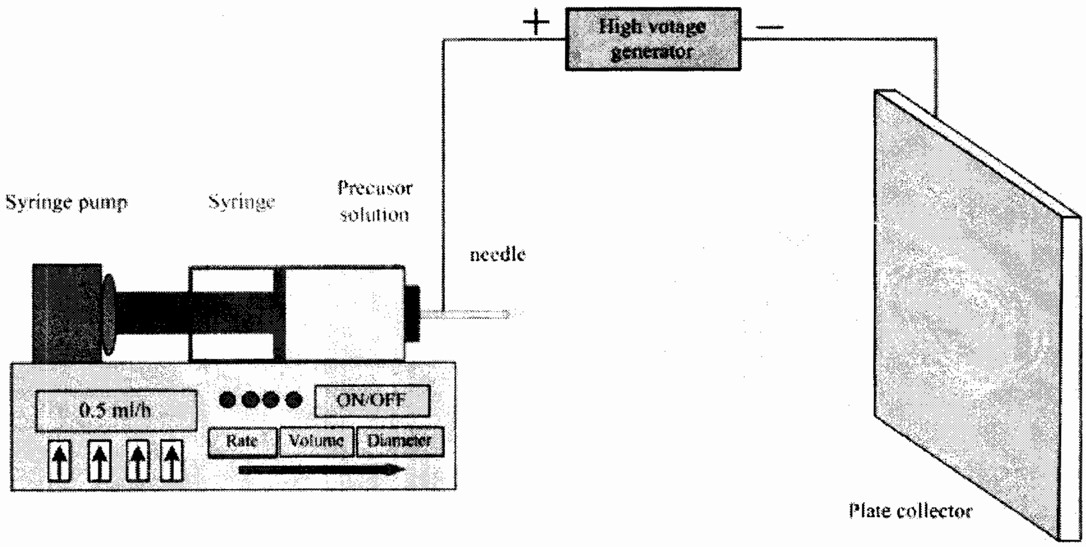

Figure 3.2 Schematic drawing of the electrospinning setup.

The forces due to electric field and gravitational field are

$$F = qE = \frac{qV}{d},$$

$$F = ma = mg,$$

while the order of magnitude of q is 10^{-19}, V is 8 x 10^{3} and d is $15\text{x}10^{-2}$ in SI units, the refore the force due to electric field is 0.2 x 10^{-14} Newton. The force of the fibers due to gravitation is $1.5\text{x}10^{-15}$ Newton which is small when compared with electromagnetic force.

3.4 Experimental Procedures

(1) Preparation of the TiO_2/PVP composite fibers

For the electrospinning process, first, the composite solution was loaded into a syringe equipped with 21-gauge stainless steel hypodermic needle. The terminal positive of a DC high-voltage power supply was attached to needle tip and the terminal negative was attached to the ground collector which was covered by aluminum foil. The distance between the needle tip and collector is fixed at 15 cm. the feed rate of composite solution was fed at a constant rate of 1 mL/h using syringe pump (New Era; NE-300). The as-spun fiber were collected on ground collector. All experiment procedure was carried out in the atmosphere ambient.

(2) Calcination of the TiO_2/PVP composite fibers

The electrospun TiO_2/PVP composite fibers were subjected to heat treatment at ranging from 500 -700 °C for 1-2 h in air by using box furnace to crystallization of TiO_2. The calcined fibers were.characterization by thermogravimetric analysis (TGA), X-ray diffraction (XRD), scanning electron microscopy (SEM), and Fourier transform infrared spectroscopy.

3.5 Characterization techniques

3.5.1 Thermogravimetery

Thermogravimetric analysis (TGA) is a complementary technique used in combinationwith FTIR analysis to probe the amount and surface coverage of nanoparticles coated with different functional groups and surfactants. TGA can be also be used to determine whether the groups attached to the surface of nanoparticles are bonded physically (e.g. via hydrogen bonding) or chemically (covalent attachment). It also helps determine the moisture content of a sample. Phase transitions, which may occur during heating, are also signaled in the final thermogram. Though there are many variants of TGA, the most general form is to subject a material to controlled heating and measure the corresponding change in mass of the material as a function of temperature. A small amount of sample, usually 10-20 mg is placed in a ceramic sample pan supported by a sensitive balance. Another empty pan supported by the same balance is used as a reference. Depending upon the nature of the sample, the temperature range may vary from 500-700°C. Temperature scan rates can be varied from 5 to 20 °C/min. The suitable temperature for calcination was carried out by including thermogravimetric analysis (TGA, Thermo plus TG8120, Rigaku Corp.) [44].

3.5.2 X-ray diffraction (XRD)

X-Ray Diffraction is usually the first and most commontechnique employed to obtain information about the crystallinity, composition, size, and symmetry of the unit cell of the solid. Each crystalline solid possess its own characteristic XRD pattern that can be used as a fingerprint for its identification. In crystalline solids, the atoms are regularly arranged in three dimensional spaces to form arrays of points that constitute the crystal lattice. These arrangements result in a series of parallel planes with various orientations and specific interplanner distances (d, approximately 1 Å). These planes can diffract electromagnetic radiations of about the same wavelengths as the interplanner spacing in the solid. X-rays with wavelengths ~1Å (1.54 Å for CuKα radiations) are therefore ideal electromagnetic radiations for diffraction studies of solids. When a focused beam of X-rays impinges on a crystal lattice at a certain angle, diffraction occurs when Bragg's condition; $n\lambda = 2d\sin\theta$ is fulfilled. Here, n = 1, 2, 3… is an integer, λ is the wavelength of X-ray radiation, and θ is the diffraction angle. The diffracted radiations are collected to construct specific diffraction patterns [45].

The XRD patterns of the samples were collected Phillip 2000 X'Pert-MPD System with CuKα radiation source (λ= 1.54 Å) was used to identify the crystal phase and estimate the crystallite size.

3.5.3 Scanning electron microscopy (SEM)

Scanning electron microscopy is a useful instrument for imaging topographies of examples at very high magnifications using electrons instead of light. Compared to traditional optical microscopes, the SEM possesses many advantages. For instance, the SEM has a larger depth of field (up to 100 times), permitting more of theexamples to be in focus at one time. Additionally, very high resolution of SEM allows the examples which are very close to each other, to be detected and magnified at much higher levels (>100,000x). Utilizing electromagnets rather than lenses in the SEM facilitates a much more control in the degree of magnification. In addition to the mentioned advantages, the scanning electron microscope provides considerably clear images, giving rise to a high efficiency for various research areas [46, 47]. While SEM inspection, a spot volume of the example is electron bombarded by an electron beam produced at the top of the microscope by an electron gun which is a thermal emission source, such as a heated tungsten filament or a field emission cathode. Depending on the inspection purpose, the incident electrons' energy varies from as low as 100 eV to as high as 30 keV.

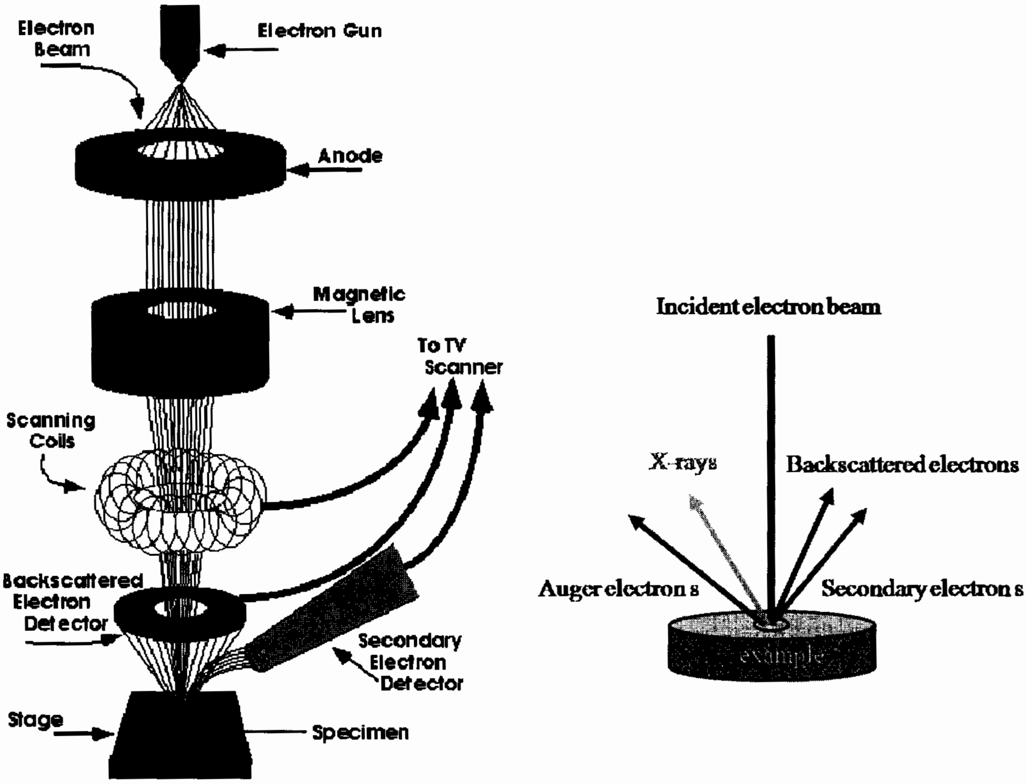

(a) (b)

Figure 3.3 (a) Schematic of the SEM and (b) electron beam-example interaction [45].

As shown in figure 3.3(a), the electron beam travels vertically (top to bottom) through the microscope and under vacuum. The electromagnetic fields and lenses present on the SEM column focus the beam down toward the sample. Finally, the scanning coils located near to the end of the column are responsible for positioning and directing the focused electron beam onto the sample surface. To image topography, the electron beam is scanned in a raster pattern over the surface [46]. As seen in figure 3.3 (b), the bombarding electrons, also known as primaryelectrons, force out the electrons of the example due to elastic and inelastic scattering events occurring at the surface and near-surface of the sample. The high-energy electrons dislodged by an elastic collision of an incident electron with a sample atom's nucleus are called backscattered electrons. This kind of electrons is as energetic as the incident electrons and in number is a function of the example's atomic number. Hence, the backscattered electron imaging could be useful in distinguishing one material from another with atomic number difference of at least 3 [46, 47]. The low energy (50 eV or less) electrons emitted by the inelastic scattering of incident electrons are called secondary electrons. In fact, secondary electrons are either those incident electrons that after collisions with the nucleus lose their energy significantly or those loosely bound electrons that eject from the sample atoms. A positively biased grid or detector collects the secondary electrons and subsequently translates them into a signal. Sweeping the electron beam across the area to be inspected results in production of many such signals which are subsequently amplified, analyzed, and translated into images of the evaluated topography [48]. As seen in figure 3.3 (a), generally two types of electron detector are utilized for SEM imaging: 1) Scintillator type detectors (for secondary and backscattered electron imaging) which are positively charged to attract electrons thereby improve signal to noise ratio and 2) solid-state detectors only for backscattered electrons [46]. As illustrated in figure 3.3(b), other sorts of signals produced by the interaction of the primary electron beam with the example are characteristic X-rays and auger electrons. When an incident electron dislodges an electron from an inner atomic shell, a vacancy is formed in that electron shell. The vacancy could be filled by an electron from an outer shell to balance the atomic orbital's following an ionization event. During this process, the filling electron loses energy as X-rays. The released characteristic X-rays are usually utilized for energy dispersive X-ray analysis. Auger electrons are released when an outer shell electron replaces an inner shell electron already dislodged by a primary or backscattered electron and fills the respective vacancy. This replacement is accompanied with release of excess energy which could be carried away by an auger electron. Owing to the equality of the energy of Auger electrons with the energy difference between the two shells, similar to X-rays an Auger electron can represent the type of element from which it was released and its respective shell energy. Auger Electron Spectroscopy for analysis of surface chemistry is based on discriminating between Auger electrons of various energies. Auger electrons due to their low energy level can be emitted only from near the surface. Possessing an escape depth of 0.5 to 2 nm, these electrons show a good potential spatial resolution close to that of the primary beam diameter [49]. The surface morphology and fiber diameter of the sampleswas analysed with a scanning electron microscope (SEM, JSM-6010LV, JEOL).

3.5.4 Fourier transform infrared (FTIR) spectroscopy

FTIR is a very useful tool used to ascertain the presence of molecular groups and coatings on the surface of nanofibers. Surface coatings are employed to prevent nanofibers from growth and aggregation as well as to modify the surface properties of inorganic nanofibers. FTIR spectroscopy takes into account the vibrational characteristics of crystals and other non-linear molecules. Atoms connected together with chemical bonds can vibrate about that bond with certain frequencies. The frequency of vibration is determined by strength of the bond and masses of the atoms attached. For molecular and crystal vibrations, the bond vibrational frequencies ranging from 10^{12} to 10^{14} Hz (λ = 2.5-50 μm) corresponds to the infrared region of the electromagnetic spectrum. Different types of vibrational modes can be distinguished such as bending, stretching, wagging, twisting, scissoring etc. Vibrations are also classified as symmetric or anti-symmetric, depending on how different stretching modes can affect the symmetry of a crystal or molecule. IR radiation from a source when fall on the sample can couple with bond oscillations and energy exchange occur when the two are in resonance. The IR spectrometer measures the frequencies absorbed by the sample and plot them as intensity-wave number output. It must be noted that only those vibrational modes are IR active that can cause a net change in the dipole moment of a molecule or crystal [50]. In the present work, samples for FTIR analysis were prepared in the characteristic FTIR transmission bands of PVP/TIP before andafter calcinations at 600°C for 1 h. Spectra in the range of 4000-400 cm^{-1} were collected in transmission mode using Perkin Elmer (1760x) Spectrum to verify the composition of the fibers from functional groups.

CHAPTER 4

RESULS AND DISCUSSION

In this study, effects of many parameters in sol gel and electrospinning process to fabricate titania nanofibers were investigated in detail to understand the correlation between electrospinning parameters and properties of the synthesized titania fibers, including morphology and phase stability of titania nanofibers. The fibers were characterized by thermogravimetric analysis (TGA), X-ray diffraction (XRD), scanning electron microscopy (SEM) and Fourier transform infrared spectroscopy (FTIR).

4.1 Calcination of the TiO_2/PVP composite fibers

Thermogravimetric analysis (TGA) of the as-spun PVP/TIP composite nanofibers was carried out in order to investigate the sample weight loss and thermal behavior during the calcinations process. The TGA temperature profile set at a heating rate of 10°C min^{-1} in oxygen gas, it found that the thermal decomposition of PVP is completed at 350°C as shown in figure 4.1. This result also agrees with the TGA curve resulting from performed on electrospun PVP/TIP composite nanofibers. The TGA curve exhibits three apparent weight losses. The first weight lossof 32%, it is observed that the weight loss below 280°C is due to the removal of traces of solvents such as water, methanol, acetic acid, carbon dioxide and so on. The second weight loss of 68% between 281 and 360°C is due to organic decomposition in conjunction with the degradation of PVP dehydration through a polymer side chain and decompositionof organic groups from the organometallic precursor (TIP). The weight loss over 360°C was almost remaining constant, indicating the formation of the TiO_2 nanofibers. Therefore, the temperature of 500–700 °C was selected as the calcination temperature to remove theorganic compound and formation the metal oxide.

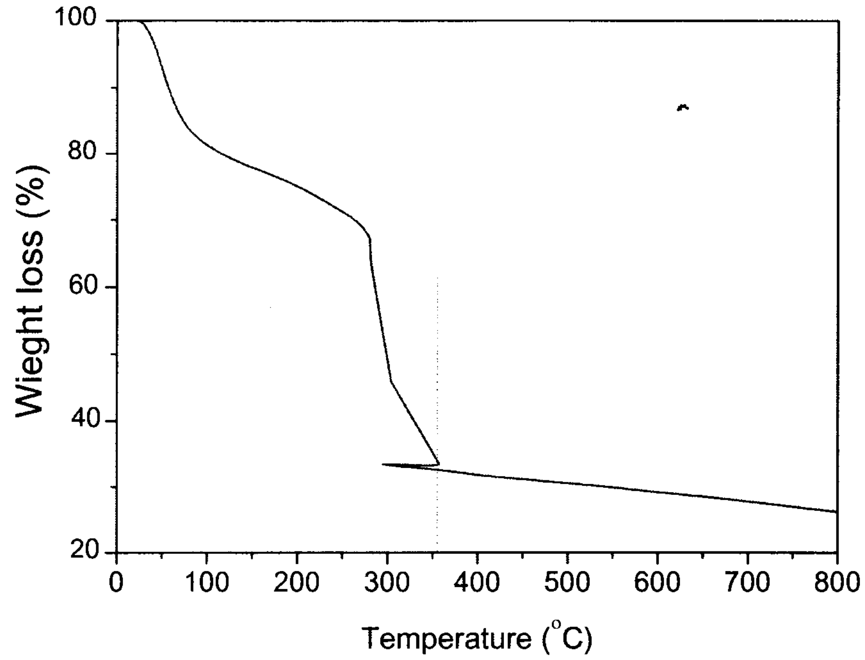

Figure 4.1 TGA curve of PVP/TIP composite nanofibers at heating rate 10°C min^{-1} in oxygen gas.

4.2 Crystal structure of thetitania nanofibers

Structural analyses of the titania nanofibers were carried out at room temperature using X-ray diffractometer (XRD). This analysis was important to verify formation of the titania nanofibers and their probable crystallinity. In figure 4.2 shows XRD patterns of PVP/TIP composite nanofibers calcined at different temperatures. Figure 4.2 (a) shows a broad peak around $2\theta = 27.21°$ corresponded to the semi-crystalline of PVP in PVP/TIP composite nanofibers. After the PVP/TIP composite nanofibers at amount of 1.0, 5.0 and 10.0 mmol were calcined at 600°C for 1 h, XRD patterns showed that PVP disappeared and the rutile TiO_2 nanofibers were formed asshown in Figure 4.2 (b–d). The XRD peaks in the wide angle range of 2θ ($10° < 2\theta < 80°$) ascertained that the peaks in 25.2°, 27.4°, 36.0°, 39.1°, 41.2°, 44.0°, 54.3°, 56.6°, 62.7°, 64.0°,68.9°, and 69.8° can be attributed to anatase phase for 25.2° the 101 (JCPDS Card no. 78-2486 and JCPDS Card no. 84-1286) and rutile phase the 110, 101, 200, 111, 210, 211, 220, 002,311, 301, and 112 crystalline structures of rutile synthesized TiO_2 nanofibers, respectively, (JCPDS Card no. 04-0551). XRD patterns showed that the crystal structure belongs to rutile TiO_2 and the anatase TiO_2 at approximately 27.4° as shown in Figure 4.2 (b–c).

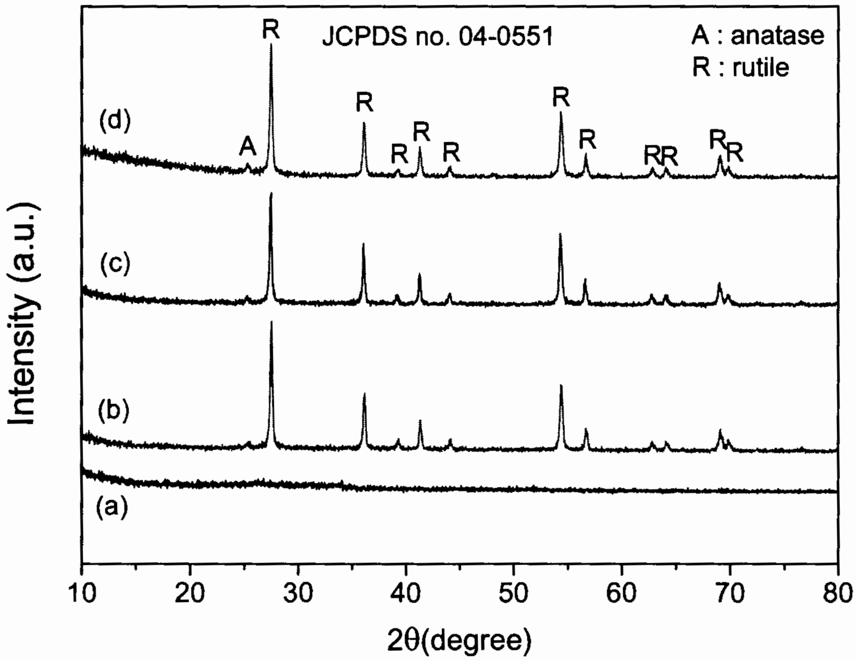

Figure 4.2 XRD patterns of (a) PVP /TIP composite nanofibers, (b) PVP/TIP1.0, (c) PVP/TIP 5.0 and (d) PVP/TIP 10 mmolcalcined at 600°C for 1 h.

As the calcination temperature increasing from 500–700°C, XRD results indicated the formation of TiO_2 corresponding to both rutile and antaste phases as shown in Figure 4.3 (a). The XRD patterns of TiO_2 nanofibers with the content of TIP 5.0 mmol calcined at 500°C shown peaks in the wide angle range of 2θ ($10° < 2\theta < 80°$) as certained that the peaks in 25.4°, 37.9°, 48.1°, 54.2°, 55.2°, 62.8°, 69.0°, and 75.2° can be assigned to 101, 004, 200, 105, 211, 204, 116, and 215 reflections of anatase (JCPDS Card No. 21-1272) and 27.5°, and 41.3° can be assigned to 110, and 210 reflections of rutile (JCPDS Card No. 21-1276), proved that the samples are crystallized in mix anatase and rutile phase.

Figure 4.3 (b) the XRD patterns of TiO_2 nanofibers with the content of TIP 5.0 mmol calcined at 600°C shown all peaks at 2θ of 25.5°, 54.5°, 62.9°, and 69.1°can be assigned to 101, 105, 204, and 116 reflections of anatase (JCPDS Card No. 21-1276) and 27.6°, 36.2°, 39.3°, 44.3°, 56.8°, 64.2°, and 69.9° can be assigned to 110, 101, 200, 210, 220, 310 and 112 reflections of rutile (JCPDS Card no. 84-1286).

Figure 4.3 (c) at 700°C shown that the peaks at 2θ of 27.6°, 36.2°, 39.4°, 41.4°, 44.2°, 54.5°, 56.8°, 62.9°, 64.2°, 68.1°, 70.0°, and 76.7°can be assigned to 110, 101, 200, 111, 210, 211, 220, 204, 310, and 112 reflections of rutile (JCPDS Card no. 84-1286).

After calcination with temperature of 600–700°C, it was revealed that the anatase phase were gradually decreased (Figure 4.3 (b)) and transformed to pure rutile phase at 700°C as shown in Figure 4.3 (c). The XRD patterns revealed an increase in the intensity of the diffraction peaks associated with increase of the calcination temperature.

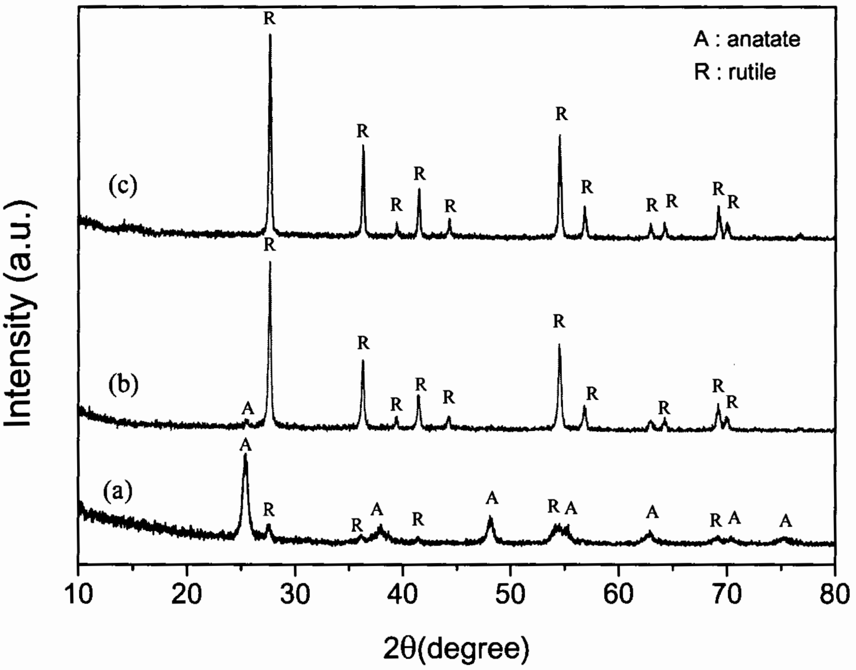

Figure 4.3 XRD patterns of TiO_2 nanofibers with the content of TIP 5.0 mmol calcined at (a) 500, (b) 600, and (c) 700°C for 2 h.

After the PVP/TIP composite nanofibers at amount of 1.0, 5.0 and 10.0mM were calcined at 600°C for 1 h. The crystallite sizes of the TiO_2 nanofibers were determined from XRD peaks of crystal structure rutile TiO_2 in figure 4.2 (b-d) by Scherrer formula [44]. The TiO_2 nanofibers crystallite of a size calculated to show the table 4.1.

Table 4.1 Calculation of the crystallite size of the PVP/TIP composite nanofibers at amount of 1.0, 5.0 and 10.0 mmol calcined at 600°C for 1 h.

sample 1.0 mmol		sample 5.0 mmol		sample 10.0 mmol	
2θ	Crystallite size (nm)	2θ	Crystallite size (nm)	2θ	Crystallite size (nm)
27.547	90.66512	25.2324	60.13214	27.6489	80.59745
36.1552	61.72862	27.4808	80.56843	36.2813	148.2272
39.2721	62.30526	36.0549	148.1315	39.4056	93.53645
41.3158	62.71463	39.1947	62.29025	41.4725	107.5534
44.1549	63.32606	41.2563	75.25557	44.2753	126.7062
54.3836	56.56492	44.0088	63.29335	54.5095	132.0276
56.6608	57.16026	54.3024	79.15632	56.8096	80.07473
62.7853	41.25753	56.6188	49.99854	62.9634	51.6177
64.1644	51.95429	62.7697	51.56435	64.2256	69.28828
69.0595	116.8516	64.0855	51.93187	68.1859	121.4748
69.8748	44.03623	68.9967	85.46891	70.0033	53.74148
		69.8273	44.02347	76.7567	30.70134

The TiO_2 nanofibers with the content of TIP 5.0 mmol calcined at 500, 600, and 700°C for 2 h, also, determined from XRD peaks of crystal structure anatase and rutile phase of TiO_2 in figure 4.3 (a-c). The TiO_2 nanofibers crystallite of a size calculated to show the table 4.2.

Table 4.2 Calculation of the crystallite size of TiO_2 nanofibers with the content of TIP 5.0 mmol calcined at 500, 600, and 700°C for 2 h.

sample 500°C		sample 600°C		sample 700°C	
2θ	Crystallite size (nm)	2θ	Crystallite size (nm)	2θ	Crystallite size (nm)
25.3681	60.14814	25.5036	60.1642	27.6489	80.59745
27.5387	36.25619	27.6251	103.5782	36.2813	148.2272
37.9415	31.03265	36.2687	123.4973	39.4056	93.53645
41.3966	31.37231	39.3731	62.3249	41.4725	107.5534
48.1759	27.55572	41.4197	53.78683	44.2753	126.7062
54.2841	19.78746	44.3129	54.32307	54.5095	132.0276
55.2524	33.1253	54.5106	56.59721	56.8096	80.07473
62.8485	25.79301	56.8355	57.20739	62.9634	51.6177
69.0629	21.37573	62.9587	51.6164	64.2256	69.28828
75.2129	18.22779	64.2703	51.98446	68.1859	121.4748
		69.1885	53.47632	70.0033	53.74148
		69.9903	44.06731	76.7567	30.70134

4.3 Surface Analysis of the titania nanofibers

The SEM images of the PVP/TIP composite fibers of as-spun nanofibers; (a) PVP/TIP 1.0 mmol, (b) PVP/TIP 5.0 mmol, (c) PVP/TIP 10.0 mmol and TiO_2 nanofibers; (d) PVP/TIP 1.0 mmol, (e) PVP/TIP 5.0 mmol, (f) PVP/TIP 10.0mmol calcined at 600°C for 1 h. The SEM micrographs of as-spun PVP/TIP composite nanofibers and TiO_2 nanofibers calcined at 600°C for 1. Figure 4.4-4.6 shows the morphologies of the as-spun fibers are random orientation and smooth surface due nature of PVP in PVP/TIP composite fibers and several micrometers in length. After calcination at high temperature, the nanofibers is smaller in diameter than the as-spun nanofibers and the surface of the fibers became rougher, which is derived from the decomposition of PVP and crystallization of TiO_2. The average diameter of as-spun PVP/TIP composite nanofibers is in range of 298–365 nm at different concentrations of TIP. After calcination at high temperature, the average fiber diameter of TiO_2 nanofibers is shrinked and the average of the fiber diameters is reduced to 147–284 nm as shown in figure 4.7-4.9. SEM images also indicate that the average of the fiber diameter is decreased as calcination temperature increases due to increasing the decomposition of PVP polymer. The result of SEM micrograph shows that the increase of TIP concentrations influences on the increase of fiber diameter of TiO_2 nanofibers. Then after the calcination at 600°C for 1 h, SEM images showed that fiber diameter is decreased as calcination temperature increases in the range of 150–300 nm.

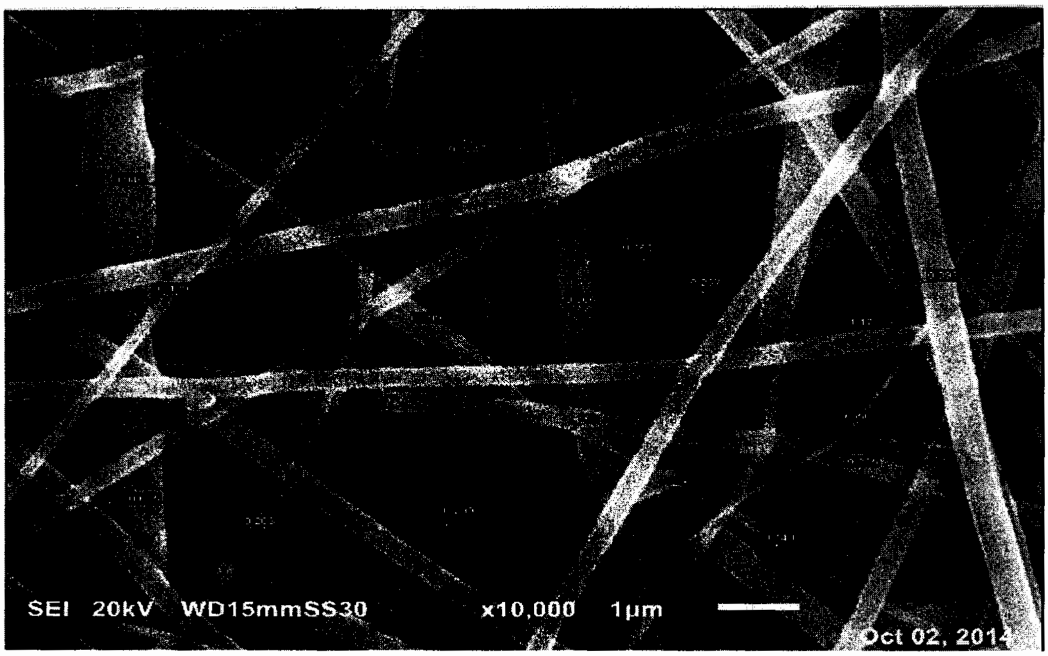

Figure 4.4 SEM images of the PVP/TIP composite fiber of as-spun nanofibers; PVP/TIP 1.0 mmol.

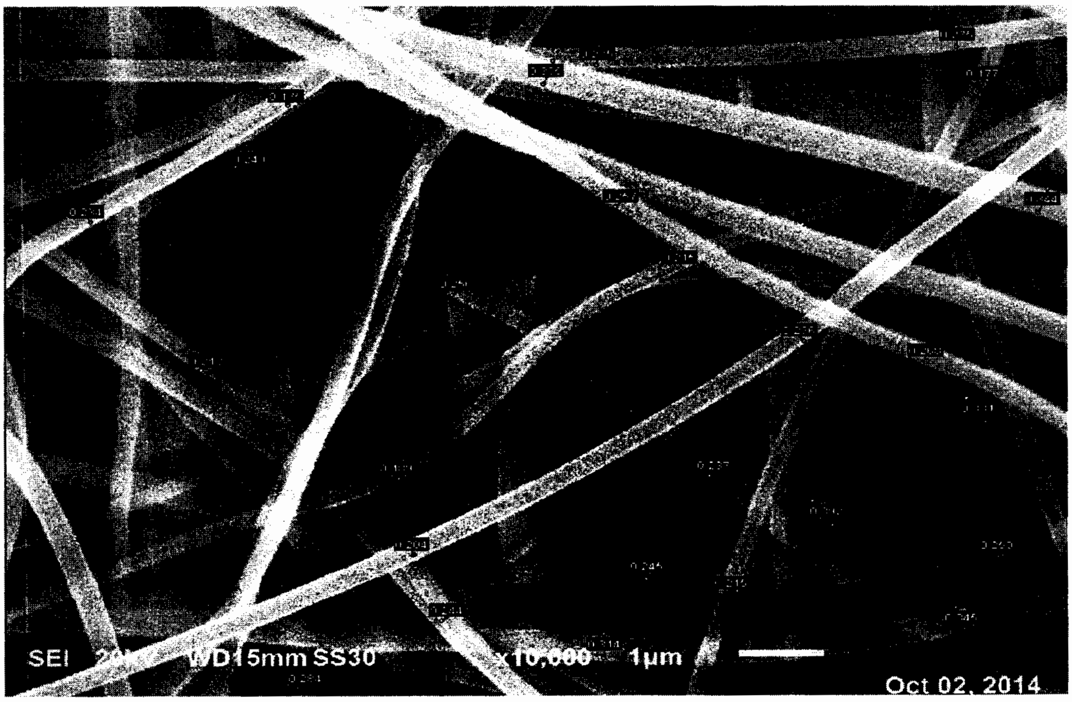

Figure 4.5 SEM images of the PVP/TIP composite fiber of as-spun nanofibers; PVP/TIP 5.0 mmol.

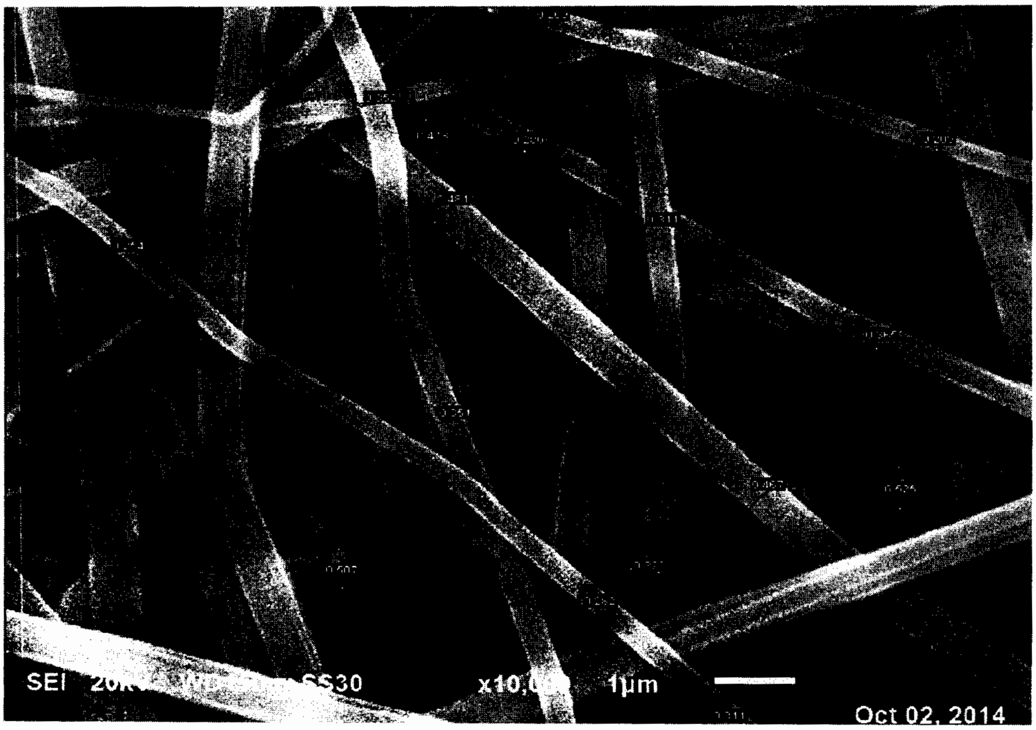

Figure 4.6 SEM images of the PVP/TIP composite fiber of as-spun nanofibers; PVP/TIP 10.0 mmol.

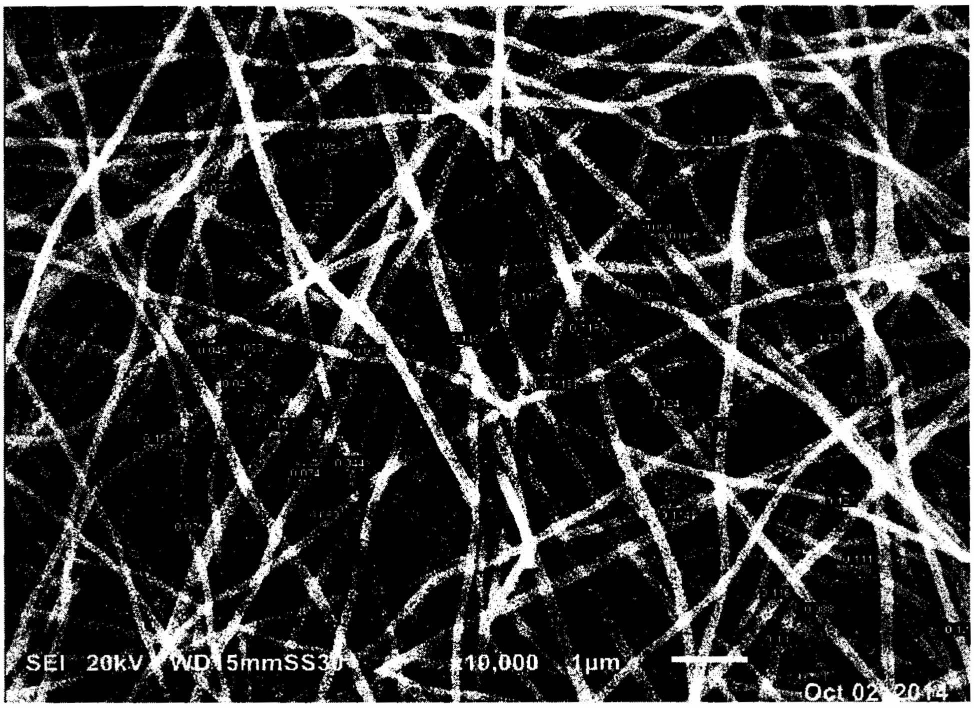

Figure 4.7 SEM images of the PVP/TIP composite fiber of as-spun nanofibers; PVP/TIP 1.0 mmol calcined at 600°C for 1 h.

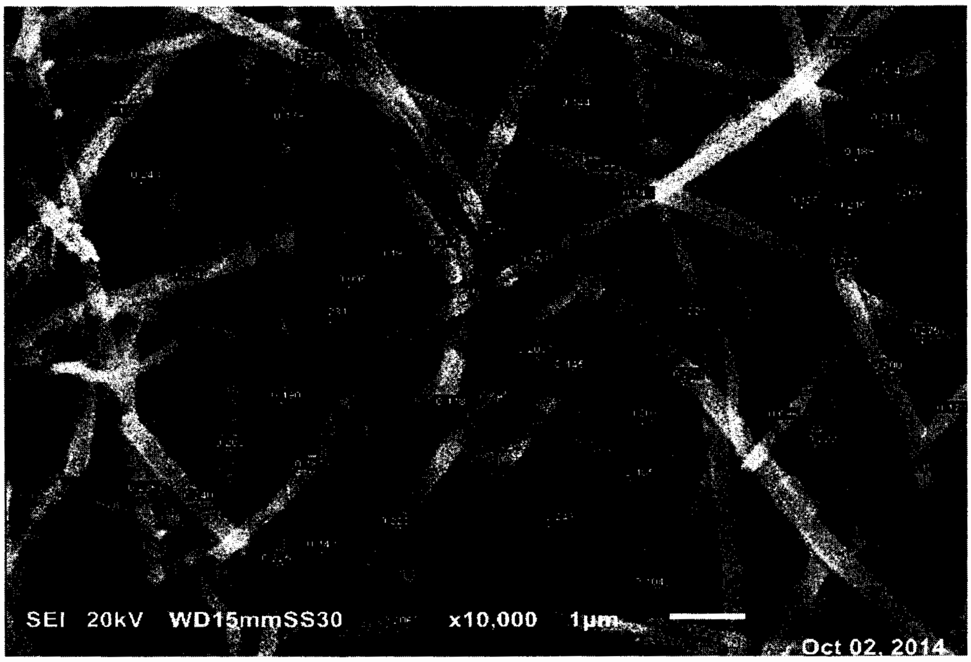

Figure 4.8 SEM images of the PVP/TIP composite fiber of as-spun nanofibers; PVP/TIP 5.0 mmol calcined at 600°C for 1 h.

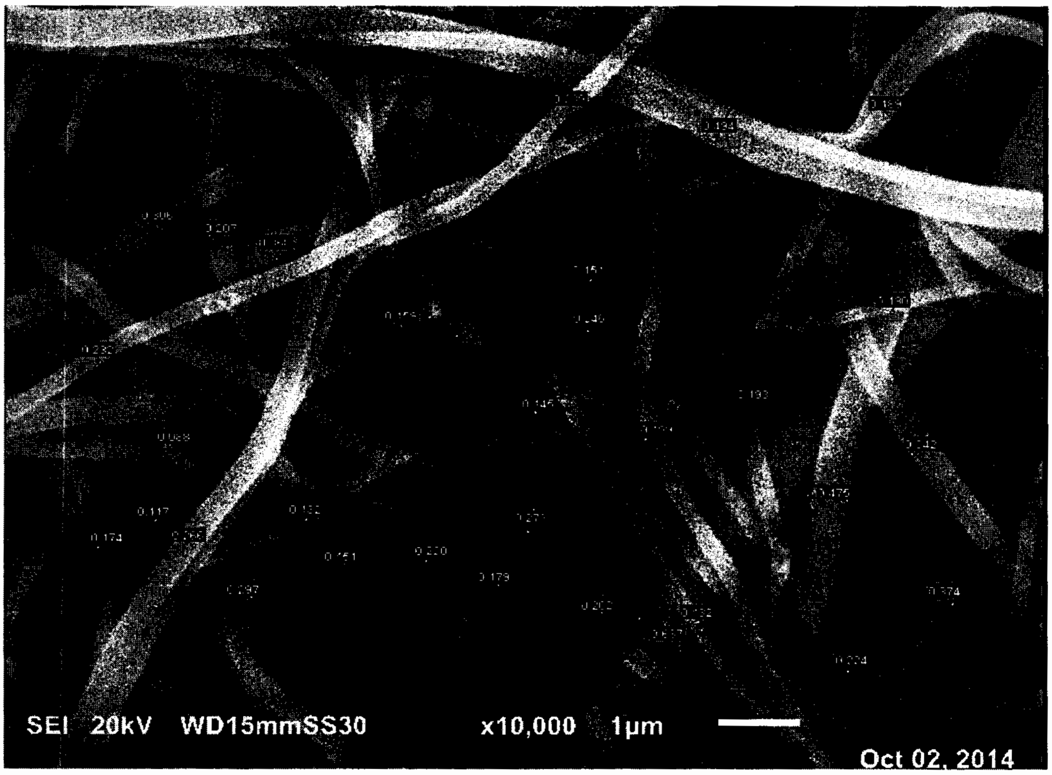

Figure 4.9 SEM images of the PVP/TIP composite fiber of as-spun nanofibers; PVP/TIP 10.0 mmol calcined at 600 °C for 1 h.

4.4 Fourier transforms infrared spectroscopy of the titania nanofibers

Fourier transform infrared spectroscopy (FTIR) analyses of different aliquots of a single sample typically produce identical spectra. In some instances, usually in samples containing higher amounts of contamination, variable spectra are observed. In this technique for FTIR analysis confirmed the presence of PVP. Figure 4.10 shows the characteristic FTIR transmission bands of PVP/TIP before and after calcinations at 600°C for 1 h. Figure 4.10 shows the characteristic FTIR transmission bands of PVP/TIP before and after calcinations at 600°C for 1 h. Figure 4.10 (a) shows a very broad band observed between 3,600 – 3,200 cm^{-1} which is linked to the hydrogen bonded O-H stretching vibration due to the presence of moisture in the composite fibers. The vibration band at approximately 2,964 cm^{-1} refers to the C-H stretching of methyl groups. The peak at 1,686 cm^{-1} can be attributed to the contribution from the C=O stretching of amide in PVP. The vibration bands at between 429 and 735 cm^{-1}

are related to C-C, C-O and C-N of PVP polymer. The peaks at 654 and 584 cm^{-1} refer to N-C=O bending.

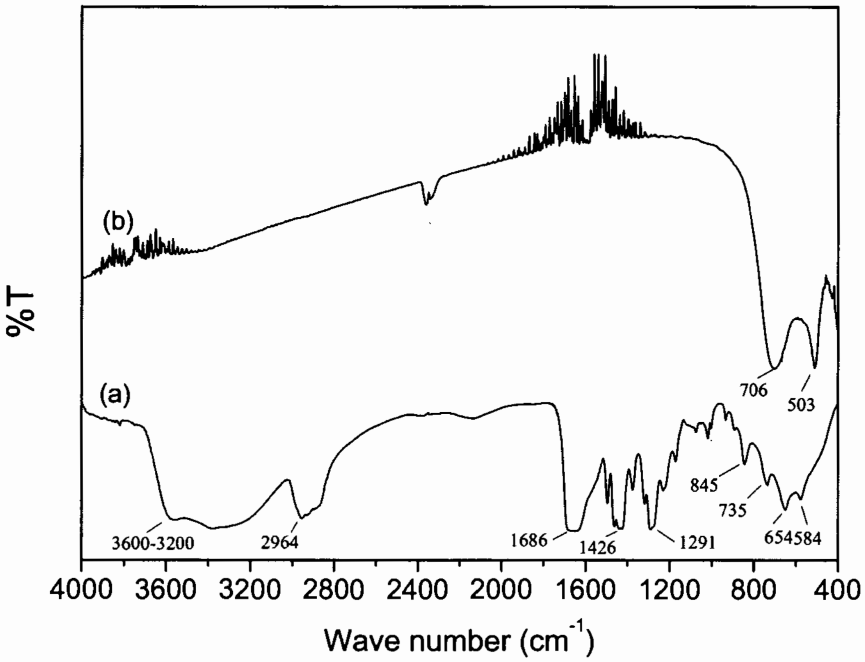

Figure 4.10 FTIR spectrums for (a) as-spun PVP/TIP nanofibers and (b) TiO_2 nanofibers calcined at 600°C for 1 h.

Figure 4.10 (b) shows a small amount of IR bands in TiO_2 nanofibers due to remaining the polymer after calcination with temperature of 600°C for 1 h. The vibration bands at 706 and 503 cm^{-1} are related to binding energy of titanium metal reacted with oxygen (Ti-O) and then formation of TiO_2 nanofibers after calcination at high temperature [51].

CHAPTER 5
CONCLUSIONS AND SUGGESTION

In this work, TiO_2 nanofibershave been synthesized by electrospinning and studied the effect of preparation parameters on the characterization such as the effects of concentrations of reacting agents (titanium tatraisopropoxide ($Ti(OCH(CH_3)_2)_4$ and glacial acetic acid, effect of calcination time, temperature, and concentration of the TiO_2/PVP.

5.1 Summary

TiO_2 the TiO_2/PVP composite fibers can be fabricated by electrospinning process followed by calcinations and concentration. Sol-gel process occurred only when using methanol as solvent in titanium dioxide precursor solution. After titanium dioxide precursor solution with methanol solvent was aged for half an hour, it was found that sol-gel process was completed. TGA curve results from performed on electrospun PVP/TIP composite nanofibers. The weight loss over 350°C was almost remaining constant, indicating that the formation of the TiO_2 nanofibers occurs. The crystallinity of rutile phase of TiO_2 nanofibers were calcined at high temperature of 700°C. The morphology of TiO_2 nanofibers by SEM micrograph shows that the increase of TIP concentrations influences on the increase of fiber diameter of TiO_2 nanofibers. The diameter of the nanofibers is decreased when the calcination temperature is increased. IR bands in TiO_2 nanofibers due to remaining the polymer after calcination with temperature of 600°C for 1 h. The vibration bands at 706 and 503 cm^{-1} are related to binding energy of titanium metal reacted with oxygen (Ti-O) and then the data confirms formation of TiO_2 nanofibers after calcination at high temperature.

5.2 Conclusions

TiO_2 nanofibers with diameters of 147 – 284 nm have been successfully synthesized by sol-gel assisted electrospinning method. The crystallinity of rutile TiO_2

was obtained after the as-spun TiO_2 fibers were calcined at high temperature and also the mixtures of anatase in rutile phase of TiO_2 nanofibers were formed. However, it was observed that the increase of the titanium isopropoxide concentration does not influence to the phase structure. The average of the diameters of TiO_2 nanofibers is increased as the titanium isopropoxide contents increased and is decreased as the calcination temperature increase.

5.3 Suggestions

Future, the fabrication should be carried out by arranging the apparatus in a vertical plane or in different angles. The sol-gel process should be used the titanium tetraisopropoxide (TIP, $Ti(OCH(CH_3)_2)_4$ was added, drop – by –drop, into a well-mixed methanol – water solution. The TiO_2 nanofibers should be prepared to use such application and the electrical properties and other properties to be studied for the dye sensitized solar cells or other devices.

REFERENCES

REFERENCES

[1] Y. Cao and et al. “Electrospun TiO_2 nanofiber based hierarchical photoanode for efficient dye-sensitized solar cells”, **Electrochimica Acta**. 189(20): 259–264; January, 2016.

[2] S. Zhuiykov, W. Wlodarski and Y.X. Li. “Nanocrystalline V_2O_5–TiO_2 thin-films for oxygen sensing prepared by sol–gel process”, **Sensors and Actuators B: Chemical**. 77(1-2): 484–490; June, 2001.

[3] M.A.K.L. Diasanayake and et al. “TiO_2 as a Low Cost, Multi Functional Material”, **Materials Today: Proceedings**. 3(1): 40-47, 2016.

[4] S. Riaz and S. Naseem. “Controlled nanostructuring of TiO_2 nanoparticles: a sol–gel approach”, **Journal of Sol-Gel Science and Technology**. 74(2): 299–309; May, 2015.

[5] B. Samran and et al. “preparation and microstructure of Titania (TiO_2) nanotube arreays by anodization method”, **Advance Materials Reseach**. 802: 104-108; August, 2013.

[6] N. Wongpisutpaisan and et al. “Titanium Dioxide Nanostructures Synthesized by Sonochemical – hydrothermal Process”, **Journal of Metals, Materials and Minerals**, 23(1): 19-24, 2013.

[7] D. Y. Lee and et al. “Titania Nanofibers Prepared by Electrospinning”, **Journal of the Korean Physical Society**. 48: 1686-1690, 2006.

[8] G.Kickelbick. **Hybrid materials**. Wiley-VCH: Verlag GmbH & Co. KGaA, 2007.

[9] J.A. Burdick and R. L. Mauck. **Biomaterials for Tissue Engineering Applications**. NewYork: springer wien, 2011.

[10] Challa S. S. R. Kumar. **Nanotechnologies for the Life Sciences**. WILEY- VCH: Verlag GmbH & Co. KGaA, 2006.

[11] B. Caratao and et al. “Properties of Electrospun TiO_2 Nanofibers”, **Journal of Nanotechnology**. 2014 (2): 5; June, 2014.

[12] S. Ramakrishna and et al. “Electrospun nanofibers”, **materialstoday**. 9: 40-50, 2006.

REFERENCES (CONTINUED)

[13] A. Haider, S. Haider and I.K. Kang. (2015). "A comprehensive review summarizing the effect of electrospinning parameters and potential applications of nanofibers in biomedical and biotechnology", **Science Direct**. http://www.sciencedirect.com/science/article/pii/ S1878535215003275. December, 2016.

[14] X. Wang, G. He, H. Fong and Z. Zhu. "Electron Transport and Recombination in Photoanode of Electrospun TiO_2 Nanotubes for Dye-Sensitized Solar Cells", **The Journal of Physical Chemistry C**. 117(4): 1641-1646; January, 2013.

[15] M. P. Das. "Mesoscopic systems in the quantum realm: fundamental science and applications", **Advance in natural science: nanoscience and nanotechnology**. 1(4): unpaged; December, 2010.

[16] Li. Shen and et al. "Hydrothermal Splitting of Titanate Fibers to Single-Crystalline TiO2 Nanostructures with Controllable Crystalline Phase, Morphology, Microstructure, and Photocatalytic Activity", **Journal of Physical Chemistry C**. 112(24): 8809–8818; May, 2008.

[17] L. Kavan, and et al. "Electrochemical and photoelectrochemical investigation of single-crystal anatase," **Journal of the American Chemical Society.** 118(28): 6716–6723; July, 1996.

[18] A. Fahmi and et al. "Theoretical analysis of the structures of titanium dioxide crystals", **Physical Review B**. 47(18): 11717-11724; May, 1993.

[19] J. F. Banfield, B. L. Bischoff and M. A. Anderson. "TiO_2 accessory minerals: coarsening, and transformation kinetics in pure and doped synthetic nanocrystalline materials", **Chemical Geology**. 110(1-3): 211–231; November, 1993.

[20] M. Landmann, E. Rauls and W.G. Schmidt. "The electric structure and optical response of rutile, anatase and brookite TiO_2", **Journal of physics: Condensed matter**. 24(19): 195503; April, 2012.

[21] M.Hu and et al. "The effects of atmosphere and calcined temperature on photocatalytic activity of TiO_2 nanofibers prepared by electrospinning", **Nanoscale Research Letters**. 8: 548; September, 2013.

REFERENCES (CONTINUED)

[22] A. S. Edelstein and R. C. Cammarata (Eds.). **Nanomaterials: Synthesis, Properties and Applications**. Bristol: Institute of Physics Publishing, 1998.

[23] C. N. R. Rao and A. K. Cheetham. "Science and technology of nanomaterials: current status and future prospects", **Journal of Materials Chemistry**. 11: 2887-2894; June, 2001.

[24] T. Zemb and et al. "Self-assembly of flat nanodiscs in salt-free catanionic surfactant solutions", **Science**. 283(5403): 816–819; Feb, 1999.

[25] M. D. Hollingsworth. "Crystal engineering: from structure to function", **Science**. 295(5564): 2410-2413; March, 2002.

[26] M. Muthukumar, C.K. Ober and E.L. Thomas. "Competing interactions and levels of ordering in self-organizing polymeric materials", **Science**. 277(5330): 1225-1232; August, 1997.

[27] W. Nuansing and et al. "Structural characterization and morphology of electrospun TiO_2 nanofibers", **Materials Science and Engineering B**. 131(1-3) : 147–155; July, 2006.

[28] C. J. Brinker and G. W. Scherer. **Sol-Gel Science: The physics and chemistry of Sol-Gel Processing**. San Diego: Academic Press,1990.

[29] H. Albetran, Y. Dong, and I.M. Low. "Characterization and optimization of electrospun TiO_2/PVP nanofibers using Taguchi design of experiment method", **Journal of Asian Ceramic Societies**. 3(3): 292–300; September, 2015.

[30] D. Y. Lee and et al. "Titania nanofibers prepared by electrospinning", **Journal of the Korean Physical Society**. 48: 1686-1690, 2006.

[31] A. Formhals. "Process and apparatus for preparing artificial S", **US Patent**. 1: 975, 504; August, 1934.

[32] A. Formhals. "Method and apparatus for spinning", **US Patent**. 2: 975, 504; August, 1939.

[33] A. Formhals. "Artificial thread and method of producing. same filed", **US patent.** 2: 187, 306; January, 1940.

REFERENCES (CONTINUED)

[34] J.S. Kim, and D. H Reneker. “Polybenzimidazole nanofiber produced by electrospinning”, **Polymer Engineering and Science**. 39(5): 849-854; May, 1999.

[35] X. Fang and DH. Reneker. “DNA fibers by electrospinning”, **Journal of macromolecular science physics B**. 36(2): 169-73, 1997.

[36] J. Doshi, D.H. Reneker. “Electrospinning process and applications of electrospun fibers”, **Journal Electrostatics**. 35(2-3): 151-160; August, 1995.

[37] G.I. Taylor. “Electrically driven jets”, **Proc R Soc London**. 313(1515): 453-475; December, 1969.

[38] Y.M. Shin and et al. “Experimental characterization of electrospinning: the electrically forced jet and instabilities”, **Polymer**. 42(25): 9955-67; December, 2001.

[39] D.H. Reneker and L. Chun. “Nanometre diameters of polymer, produced by electrospinning”, **Nanotechnology**. 7(3): 216-223, 1996.

[40] K. S., Athira, P. Sanpui and K. Chatterjee. “Fabrication of poly (caprolactone) nanofibers by electrospinning”, **Journal of polymer and biopolymer physics chemistry**. 2(4): 62-66; November, 2014.

[41] D. Li and Y. Xia. “Fabrication of titania nanofibers by electrospinning”, **Nano letter**. 3: 555-560; March, 2003.

[42] J. Watthanaarun, V. Pavarajarn and P. Supaphol. “Titanium (IV) oxide nanofibers by combined sol-gel and electrospinning techniques: preliminary report on effects of preparation conditions and secondary metal dopant”, **Science and technology of advanced materials**. 6(3-4): 240-245, 2005.

[43] S. Madhugiri and et al. “Electrospun mesoporous titanium dioxide fibers”, **Microporous and mesoporous materials**. 69(1-2): 77-83; April, 2004.

[44] S. K. Zain. **Catalytic depolymerization of cellulose to nanocellulose using heterheteropoly acid**. Kuala lupur: University of Malaya Kuala lupur, 2015.

REFERENCES (CONTINUED)

[45] Loi de Bragg. "Bragg's law", **X-ray Diffraction**. http://www.hyperphysics.phy-astr.gsu.edu. November 25, 2010.

[46] D. McMullan. "Scanning electron microscopy 1928–1965", **Scanning**. 17: 175-185, 2006.

[47] K.C.A. Smith and C.W. Oatley. "The scanning electron microscope and its fields of application", **British Journal of Applied Physics**. 6(11): 391-399, 1955.

[48] Carol Shelby and et al. "How does a SEM work", **Scanning Electron Microscope**. https://www.purdue.edu/ehps/rem/rs/sem.htm.
October 13, 2014.

[49] Russell and et al. "scanning electron microscopy of observations on deembedded biological tissues sections: Comparison of different fixative and embedding material", **Journal of electron microscopy technique**. 2(5):489-459, 1985.

[50] A.B. Al-Zubaidi. "Scanning Electron Microscopy (SEM)", **Scanning Electron Microscopy**. http://www.Uotechnology.edu.iq/dep-material/lecture/thirdclass/characterization and test material engineerin08.pdf.
April 20, 2010.

[51] A. Patterson. "The Scherrer Formula for X-Ray Particle Size Determination", **Physical review**. 56(10): 978-982; November, 1939.

[52] B. Sahoo, and P.K. Panda. "Preparation and characterization of Barium Titanate nanofibers by electrospinning", **Ceramics International**. 38(6): 5189-5193; August, 2012.

APPENDIX

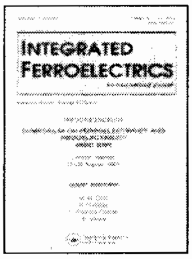

Taylor & Francis

Integrated Ferroelectrics

An International Journal

ISSN: 1058-4587 (Print) 1607-8489 (Online) Journal homepage: http://www.tandfonline.com/loi/ginf20

Preparation and Characterization of Electrospun TiO_2 Nanofibers via Electrospinning

Sert Kiennork, Ronariddh Nakhowong, Romteera Chueachot & Udom Tipparach

To cite this article: Sert Kiennork, Ronariddh Nakhowong, Romteera Chueachot & Udom Tipparach (2015) Preparation and Characterization of Electrospun TiO_2 Nanofibers via Electrospinning, Integrated Ferroelectrics, 165:1, 131-137, DOI: 10.1080/10584587.2015.1063915

To link to this article: http://dx.doi.org/10.1080/10584587.2015.1063915

Published online: 22 Oct 2015.

Submit your article to this journal

Article views: 8

View related articles

View Crossmark data

Full Terms & Conditions of access and use can be found at
http://www.tandfonline.com/action/journalInformation?journalCode=ginf20

Download by: [T&F Internal Users], [Sherry Howard] **Date:** 20 November 2015, At: 06:03

Integrated Ferroelectrics, 165:131–137, 2015
Copyright © Taylor & Francis Group, LLC
ISSN: 1058-4587 print / 1607-8489 online
DOI: 10.1080/10584587.2015.1063915

Taylor & Francis
Taylor & Francis Group

Downloaded by [T&F Internal Users], [Sherry Howard] at 06:03 20 November 2015

Preparation and Characterization of Electrospun TiO_2 Nanofibers via Electrospinning

SERT KIENNORK,[1] RONARIDDH NAKHOWONG,[2]
ROMTEERA CHUEACHOT,[3] AND UDOM TIPPARACH[1,*]

[1]Department of Physics, Faculty of Science, Ubon Ratchathani University, Ubon Ratchathani 34190, Thailand
[2]Program of Physics, Faculty of Science, Ubon Ratchathani Rajabath University, Ubon Ratchathani 34000, Thailand
[3]Program of Chemistry, Faculty of Science, Ubon Ratchathani Rajabath University, Ubon Ratchathani 34000, Thailand

In this work, titanium dioxide (TiO_2) nanofibers were synthesized by a combination of electrospinning and calcinations process using a solution that contained poly(vinyl pyrolidone)(PVP) and titanium isopropoxide. Titanium isopropoxide/PVP composite fibers were investigated at different titanium isopropoxide concentrations and voltages. The fibers were characterized by thermogravimetric analysis (TGA), Fourier transform infrared spectroscopy (FTIR), X-ray diffraction (XRD), and scanning electron microscopy (SEM). SEM images showed that the morphology of as-spun TiO_2 nanofibers are smooth, uniform and good continuous fiber morphology with fiber diameters of 150–290 nm when calcined of 600°C for 1 h in air. XRD patterns revealed that the crystallinity corresponded to TiO_2 in the form of rutile structure. The fiber diameters were slightly decreased with increase of the applied voltages and the titanium tetraisopropoxide concentration.

Keywords Titanium dioxide; sol-gel method; electrospinning; rutile structure

1. Introduction

In recent years, nanoscale one dimensional nanostructures such as nanorods, nanotubes, nanowires, nanowhiskers, nanofibers have stimulated great interest due to large surface area-to-volume ratio, high specific surface areas, small pore size and superior mechanical and electrical properties [1–3]. In order to obtain these materials, various preparation methods have been developed including discharge plasma, laser ablation, hydrothermal process and other methods. Among intensive methods for producing nanostructures, electrospinning is a very simple and convenient method for making of nanofibers. Basically, an electrospinning system consists of three major components: a high voltage power supply, a spinneret with a metallic needle, and a grounded collecting plate [4]. In the electrospinning methods, a polymer solution is placed in a syringe with a stainless steel needle and charged using a high voltage power supply. Once the electric field reaches the critical value at which the repulsive

---

Received December 22, 2014; in final form May 22, 2015.

*Corresponding author. E-mail: udomt@hotmail.com

Color versions of one or more of the figures in the article can be found online at www.tandfonline.com/ginf.

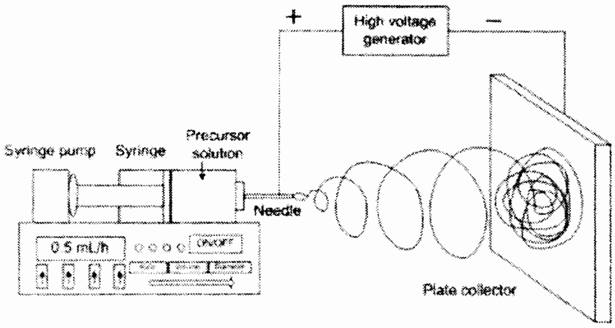

Figure 1. Schematic drawing of the electrospinning setup.

electric force overcomes the surface tension of polymer solution, the polymer solution is ejected from the tip to a collector. The ejected polymer from needle tip was deposited on the grounded collector, the electrospun material solidifies due to the fast evaporation of the solvent and with diameter raging from hundreds of nanometers to several micrometers. Titanium dioxide (TiO_2) or titania has been extensively used in many applications such as photocatalysis, gas sensors, optical filters, environmental cleaning and protection, solar cells and batteries [5]. TiO_2 has three crystalline phases; anatase, rutile and brookite. The band gap energy of anatase, rutile and brookite are 3.2, 3.0 and 1.9 eV, respectively [6–7]. The various methods for synthesis of TiO_2 include sol-gel, dip-coating, electrochemical, sputtering and chemical vapor deposition [8]. To date, one dimensional nanometerials have been successfully synthesized by various techniques. Among these the electrospinning technique has been considered to be a simple, versatile and convenient method due to its characteristics of easy control and low cost [7]. TiO_2 nanofibers were reported in various works in different precursors and electrospinning conditions [5, 8–17]. In this work, we report on the fabrication of electrospun TiO_2 nanofibers by electrospinning and calcination processing with different concentrations of titanium tetraisopropoxide, applied voltages and calcination temperatures. The titanium tetraisopropoxide and poly(vinyl pyrrolidone) were used as precursors. The morphology and crystallinity of nanofibers synthesized at different precursors, applied voltages, and calcination temperatures were investigated.

2. Experimental Details

The TiO_2 nanofibers were fabricated as follows. Based on a sol-gel processing, 1.0 mmol of titanium tetraisopropoxide (TIP, $Ti(OCH(CH_3)_2)_4$, Aldrich) was dissolved in 4 mL of glacial acetic acid and 10 mL of methanol with stirring at room temperature for half an hour to get clear solution. To this solution, 1.12 g of poly(vinyl pyrolidone) (PVP)($(C_6H_9NO)_n$, $M_w = 1{,}300{,}000$ Aldrich) was added in TIP solution and then stirred until a viscous and transparent solution wes obtained. Then, PVP/TIP was prepared with 5.0 and 10.0 mmol by using the same method as described above to obtain PVP/TIP solution. PVP/TIP solution was loaded into a plastic syringe equipped with a needle of 21-gauge. The needle made of stainless steel was connected to the terminal positive of a high voltage power supply(Gamma High Voltage ES30P) and the negative terminal of the high voltage power supply was connected to grounded collector as shown in Figure 1. The aluminum sheet used to collect the nanofibers was fastened to the grounded copper metal plate. The distance between the

Downloaded by [T&F Internal Users], [Sherry Howard] at 06:03 20 November 2015

Downloaded by [T&F Internal Users], [Sherry Howard] at 06:03 20 November 2015

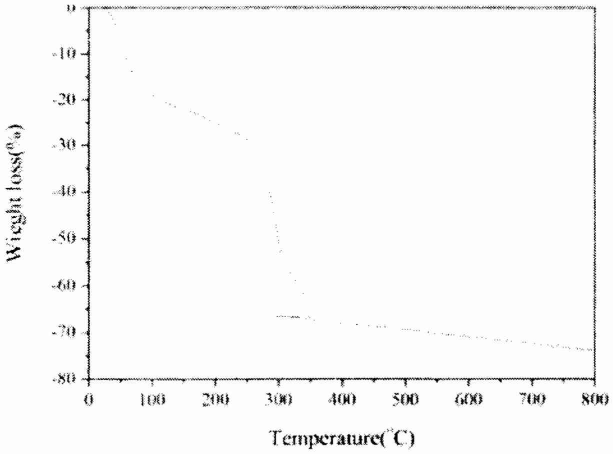

Figure 2. TGA curves of PVP/TIP composite nanofibers at heating rate 10°C min^{-1} in oxygen gas.

needle and grounded collector was fixed at 15 cm and the solution was fed at a constant rate of 1 mL/h using syringe pump (New Era; NE-300). The voltage of 8 kV was applied between the needle tip and grounded collector. All electrospinning process was carried out at room temperature in air. The electrospun PVP/TIP composite nanofibers were calcined at 500–700°C for 1–2 h in air to remove PVP and to obtain the TiO_2 nanofibers. The three types of PVP/TIP solutions with different TIP concentrations were made and studied in this work, named PVP/TIP1.0, PVP/TIP5.0 and PVP/TIP10.0 refers to different TIP concentrations of 1.0, 5.0 and 10.0 mmol.

The suitable temperature for calcination was carried out by including thermogravimetric analysis (TGA, Thermo plus TG8120, Rigaku Corp.). The crystallinity and morphology were characterized by X-ray diffraction (XRD, X' Pert 2000, Philips) and scanning electron microscope (SEM, JSM-6010LV, JEOL), respectively.

3. Results and Discussion

Figure 2 shows TGA curve resulting from performed on electrospun PVP/TIP composite nanofibers. The TGA curve exhibits three apparent weight losses. The first weight loss of 32%, it is observed that the weight loss below 280°C is due to the removal of traces of solvents such as water, methanol, acetic acid, carbon dioxide and so on. The second weight loss of 68% between 281 and 360°C is due to organic decomposition in conjunction with the degradation of PVP dehydration through a polymer side chain and decomposition of organic groups from the organometallic precursor (TIP). The weight loss over 360°C was almost remaining constant, indicating the formation of the TiO_2 nanofibers. Therefore, the temperature of 500–700°C was selected as the calcination temperature to remove the organic compound and formation the metal oxide.

Figure 3 shows XRD patterns of PVP/TIP composite nanofibers calcined at different temperatures. Figure 3(a) shows a broad peak around $2\theta = 27.21°$ corresponded to the semi-crystalline of PVP in PVP/TIP composite nanofibers. After the PVP/TIP composite nanofibers at amount of 1.0, 5.0 and 10.0 mmol were calcined at 600°C for 1 h, XRD patterns showed that PVP disappeared and the rutile TiO_2 nanofibers were formed as

Downloaded by [T&F Internal Users], [Sherry Howard] at 06:03 20 November 2015

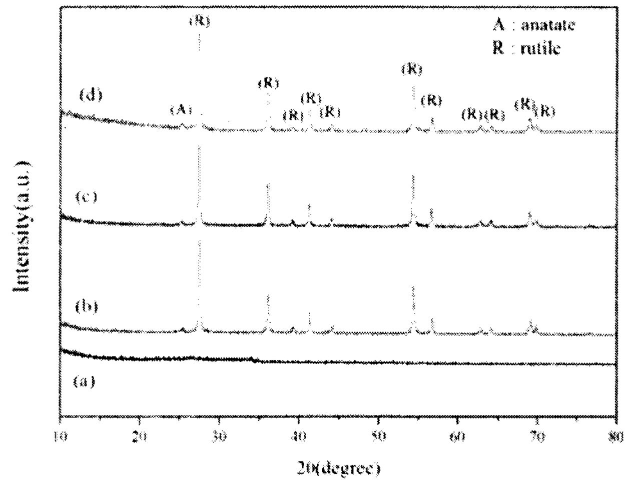

Figure 3. XRD patterns of (a) PVP /TIP composite nanofibers, (b) PVP/TIP1.0, (c) PVP/TIP 5.0 and (d) PVP/TIP 10 mmol calcined at 600°C for 1 h.

shown in Figure 3(b–d). XRD patterns showed that the crystal structure belongs to rutile TiO$_2$ and the anatase TiO$_2$ at approximately 27.51° as shown in Figure 3(b–c). As the calcination temperature increasing from 500–700°C, XRD results indicated the formation of TiO$_2$ corresponding to both rutile and antaste phases as shown in Figure 5(a). After calcination with temperature of 600–700°C, it was revealed that the anatase phase were gradually decreased (Figure 5(b)) and transformed to pure rutile phase at 700°C as shown in Figure 4(c). The XRD patterns revealed an increase in the intensity of the diffraction peaks associated with increase of the calcination temperature.

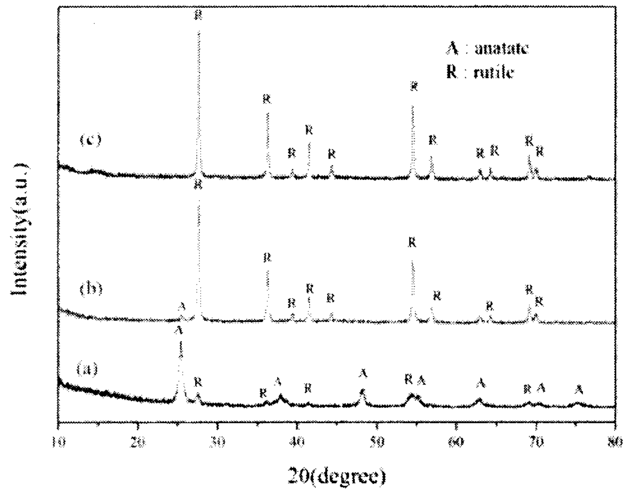

Figure 4. XRD patterns of TiO$_2$ nanofibers with the content of TIP 5.0 mmol calcined at (a) 500, (b) 600, and (c) 700°C for 2 h.

Downloaded by [T&F Internal Users], [Sherry Howard] at 06:03 20 November 2015

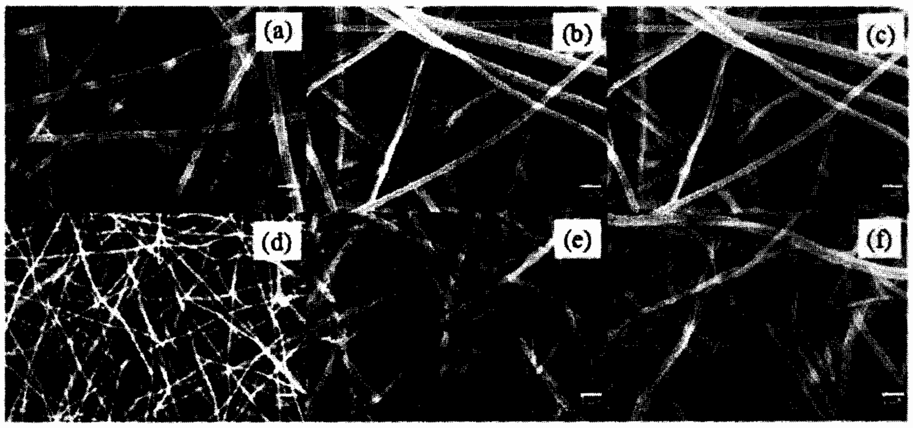

Figure 5. SEM images of the PVP/TIP composite fiber of as-spun nanofibers; (a) PVP/TIP 1.0, (b) PVP/TIP 5.0, (c) PVP/TIP 10.0 and TiO_2 nanofibers; (d) PVP/TIP 1.0, (e) PVP/TIP 5.0 , (f) PVP/TIP 10.0 calcined at 600°C for 1 h.

Figure 5 shows the SEM micrographs of as-spun PVP/TIP composite nanofibers and TiO_2 nanofibers calcined at 600°C for 1. Figure 5 (a–c) shows the morphologies of the as-spun fibers are random orientation and smooth surface due nature of PVP in PVP/TIP composite fibers and several micrometers in length. After calcination at high temperature, the nanofibers is smaller in diameter than the as-spun nanofibers and the surface of the fibers became rougher, which is derived from the decomposition of PVP and crystallization of TiO_2. The average diameter of as-spun PVP/TIP composite nanofibers is in range of

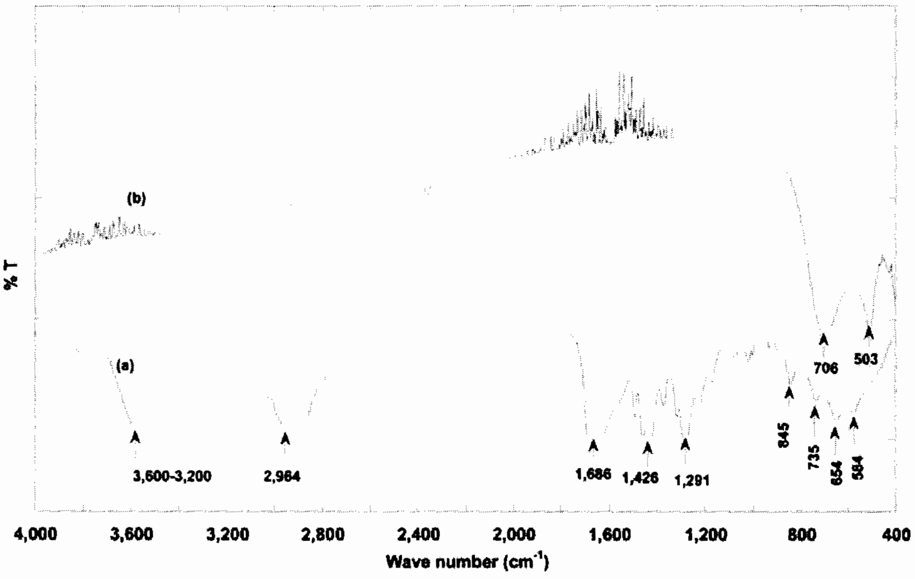

Figure 6. FTIR spectrums for (a) as-spun PVP/TIP nanofibers and (b) TiO_2 nanofibers after calcined at 600°C for 1 h.

Downloaded by [T&F Internal Users], [Sherry Howard] at 06:03 20 November 2015

298–365 nm at different concentrations of TIP. After calcination at high temperature, the average fiber diameter of TiO_2 nanofibers is shrinked and the average of the fiber diameters is reduced to 147–284 nm as shown in Figure 5(c–d). SEM images also indicate that the average of the fiber diameter is decreased as calcination temperature increases due to increasing the decomposition of PVP polymer. The result of SEM micrograph shows that the increase of TIP concentrations influences on the increase of fiber diameter of TiO_2 nanofibers. The applied voltages of 8, 10 and 12 kV which were used to PVP/TIP5.0 solution yield the diameters of the fibers were decreased from 376, 323 and 289 nm respectively. Then after the calcination at 600°C for 2 h, SEM images showed that fiber diameter is decreased as calcination temperature increases in the range of 150–300 nm (not shown).

Figure 6 shows the characteristic FTIR transmission bands of PVP/TIP before and after calcinations at 600°C for 1 h. Figure 6(a) shows a very broad band observed between 3,600–3,200 cm^{-1} which is linked to the hydrogen bonded O—H stretching vibration due to the presence of moisture in the composite fibers. The vibration band at approximately 2,964 cm^{-1} refers to the C—H stretching of methyl groups. The peak at 1,686 cm^{-1} can be attributed to the contribution from the C=O stretching of amide in PVP. The vibration bands at between 1,429 –735 cm^{-1} are related to C—C, C—O and C—N of PVP polymer. The peaks at 654 and 584 cm^{-1} refer to N-C=O bending. Figure 6(b) shows a small amount of IR bands in TiO_2 nanofibers due to remaining the polymer after calcination with temperature of 600°C for 1 h. The vibration bands at 706 and 503 cm^{-1} are related to binding energy of titanium metal reacted with oxygen (Ti—O) and then formation of TiO_2 nanofibers after calcination at high temperature [18].

4. Conclusion

TiO_2 nanofibers with diameters of 150–290 nm have been successfully synthesized by sol-gel assisted electrospinning method. The crystallinity of rutile TiO_2 was obtained after the as-spun TiO_2 fibers were calcined at high temperature and also the mixtures of anatase in rutile phase of TiO_2 nanofibers were formed. However, it was observed that the increase of the titanium isopropoxide concentration does not influence to the phase structure. The average of the diameters of TiO_2 nanofibers is increased as the titanium isopropoxide contents increased and is decreased as the calcination temperature and applied voltages increase.

Acknowledgments

This work has been supported by Program of Physics, Faculty of Science, Ubon Ratchathani Rajabhat University.

References

1. T. Zhai, and J. Yao, *One-Dimensional Nanostructures: Principle and Applications*. John Wiley & Sons, Inc, New Jersey, (2013).
2. Z. M. Wang, *One-Dimensional Nanostructures*. Springer, New York, (2008).
3. V. N. T. Kuchibhatla, A. S. Karakoti, D. Bera, and S. Seal, One Dimensional Nanostructured Materials. *Prog. Mater. Sci.* **52**, 699–913 (2007).
4. N. Bhardwaj, and S. C. Kundu, Electrospinning: A Fascinating Fiber Fabrication Technique. *Biotechnolo. Adv.* **28**, 325–347 (2010).
5. C. Tekmen, A. Suslu, and U. Cocen, Titanium Nanofibers Prepared by Electrospinning. *Mater. Lett.* **62**, 4470–4472 (2008).

6. H. S. M. Tabaei, M. Kazemeini, and M. Fattahi, Preparation and Characterization of Visible Light Sensitive Nanotitnium Dioxide Photocatalyst. *Sci. Iran.* **19**(6), 1626–1631 (2012).
7. R. Zallen, and M. P. Moret, The Optical Absorption Edge of Brookite TiO_2. *Solid State Commun.* **137**, 154–157 (2006).
8. B. Ding, C. K. Kim, H. Y. Kim, M. K. Seo, and S. J. Park, Titanium Dioxide Nanofiber Prepared by using Electrospinning Method. *Fiber and Polymer*, **5**(2), 105–109 (2004).
9. D. Y. Lee, B.Y. Kim, S.J. Lee, M.H. Lee, Y. S. Song, and J. Y. Lee, Titania Nanofibers Prepared by Electrospinning. *J Korean Phys S.* **48**(6), 1686–1690 (2006).
10. K. Onozuka, B. Ding, Y. Tsuge, T. Naka, M. Yamazaki, S. Sugi, S. Ohno, M. Yoshikawa, and S. Shiratori, Electrospinning Processed Nanofibrous TiO_2 Membranes for Photovoltaic Applications. *Nanotechnology* **17**, 1026–1031 (2006).
11. M.V. Reddy, R. Jose, T. H. Teng, B.V. R. Chowdari, and S. Ramakrishna, Preparation and Electrochemical Studies of Electrospun TiO_2 Nanofibers and Molten Salt Method Nanopaticles. *Electrochim Acta* **55**, 3109–3117 (2010).
12. W. Nuansing, S. Ninmuang, W. Jarenboon, S. Meansiri, and S. Seraphin, Structural Characterization and Morphology of Electrospun TiO_2 Nanofibers. *Mater. Sci. Eng. B-Adv.* **131**, 147–155 (2006).
13. F. Memarian, M. Latifi, and M. A. Tehran, Innovative Method for Electrospinning of Continuous TiO_2 Nanofiber Yarns: Importance Auxiliary Polymer and Solvent Selection. *J. Ind. Eng. Chem.* **20**, 1886–1891 (2014).
14. S. Madhugiri, B. Sun, P. G. Smirniotis, J. P. Ferraris, and K. J. Balkus, Electrospun Mesoporous Titanium Dioxide Fibers. *Micropor. Mesopor. Mat.* **69**, 77–83 (2004).
15. D. Li, and Y. Xia, Fabrication of Titania Nanofibers by Electrospinning. *Nano. Lett.* 3(4), 555–560 (2003).
16. K. I. Choi, S. H. Lee, J. Y. Park, D. Y. Choi, C. H. Hwang, I. H. Lee, and M. H. Chang, Fabrication and Characterization of Hollow TiO_2 Fibers by Microemulsion Electrospinning for Photocatalytic Reactions. *Mater. Lett.* **112**, 113–116 (2013).
17. S. J. Doh, C. Kim, S. G. Lee, S. J. Lee, and H. Kim, Development of Photocatalytic TiO_2 Nanofibers by Electrospinning and Its Application to Degradation of Dye Pollutants. *J. Hazard. Mater.* **154**, 118–127 (2008).
18. B. Sahoo, and P.K. Panda, Preparation and Characterization of Barium Titanate Nanofibers by Electrospinning. *Ceram Int.* **38**, 5189–5193 (2012).

Downloaded by [T&F Internal Users], [Sherry Howard] at 06:03 20 November 2015

CURRICULUM VITAE

NANE	Mr. Sert Kiennork
EDUCATION	1987 B.Ed. (physics) Teacher College Nakhon Ratchasima 1996 M.S. (Teaching Physics) Chiang Mai University
PUBLICATION	Sert Kiennork, Ronariddh Nakhowong, Romteera Chueachot and Udom Tipparach. “Preparation and TiO_2 Nanofibers via Electrospinning”, Integrated Ferroelectrics. 165: 131–137, 2015
CURRENT LOCATION	Ubon Ratchathani Rajabhat University 2 Ratchathani Road, Mueang Distric,Ubon Ratchathani Province, 34000, Thailand

Library